國立臺灣大學生命科學學院植物科學研究所

碩士論文

Institute of Plant Biology

College of Life Science

National Taiwan University

Master Thesis

鈣離子依賴磷酸激脢參與在植物先天性免疫反應以及

荷爾蒙相關防禦反應之功能性分析

Functional Characterization of CPK7 in Pattern-Triggered

Immunity and Hormone-Related Plant Defense

陳太一

Tai-I Chen

指導教授：金洛仁 博士

Advisor: Laurent Zimmerli, Ph.D.

中華民國 105 年 1 月

January 2016

誌謝

　　真正完成口試之前，總好傻好天真的以為、當你/我看到誌謝這兩個字出現的同時，一個嶄新的生命已經鋪天蓋地的在我面前展開！然而十分遺憾的(殘念！是齁！)，心裡獲得的舒坦與成就感、至多像是下午一點二十清理完垃圾回收的職日生，連插完 tip 的輪值都比不上──大概就是一種似甘蔗渣的無聊空虛吧，啊。不就跟這個學位一樣嗎？開玩笑的丂丂。然而，就算主觀上最終綜合如此，實踐上，屏除一些未被察覺目的以，客觀還是有許多值得感覺、或者感謝的事。

　　首先當然要感謝指導老師，金洛仁老師，非常非常感謝。如果沒有他，我們怎麼可能知道這份學位真正的價值呢？這種獨一無二的經驗，貨真價實的人生歷練，都是大學時期被專題老師各種呵護甚至吹捧的我無從知曉的。如果能夠與麥克阿瑟分享這種種心路歷程，為子祈禱文大概就變成了：「主啊！請讓我的孩子滿懷對生命科學的熱愛加入金洛仁老師的實驗室。」不論如何，身為敦厚老實的呆灣郎，還是非常感謝老師許多方面的指導，尤其最後改論文以及人生方面；對我而言，最後這份學位實質上更豐沛的、是管理學院的內涵。千言萬語，不及一句感謝，就像老鼠愛大米、南無阿密陀佛。

　　在實驗室的兩年時間絕對是大學時難以想像的。前一年，敏原、子娟、Cecile、郁欣、Jimmy、奕睿，還有鈺鴻、堯堯兩個神主牌，除了喜愛之外，更多的是如火一般的尊敬。碩二開始覺得可以恣意對待他人了，小麥、貝爾、安博，你們的出現實在恰如其分(就像你們在彼此的關係當中各司其職，科科)，雖然對我意義各有不同、但沒想到自己也可以這樣喜歡接近別人呢。

　　對於泰元、靜松、Eric，當然還有友慧，謝謝你們。因為我不是暴露狂，所以一如往常，對於最重要的你們、這些最重要的點滴我會一字不提。封入箱子，深深地埋在白茫茫的雲海裡。謝謝你們。

　　感謝總統卡神、James，還有口桀，有你們在身邊、讓我時時刻刻鞭策自己、活著不僅僅是活著。家銘、大凱，堉嘉；資質、變態，猴子。這些奇妙的三位一體，緊密連結著彼此，難道不就是足底根植的、無與倫比的蘭陽平原還有龜山島？嘿！我們不需要說什麼謝不謝的吧！

　　在掙扎之中，我還是想感謝 Liebe Gloyia；還有一起走過、度過好多、最可愛特別的時鐘發明者，願有一天都能光著腳、快樂的走跳於開滿小白花的草原上。還有 CPK7，謝謝你的陪伴，也希望我夠謹慎堅強、沒有讓你因愚昧疏忽等垃圾人類的垃圾理由被錯誤的理解。

　　Lieber Hermann Hesse、Heine、Kant、Beethoven、Bartok、Wagner、Shostakovich、Furtwängler Coltrane und Schubert. Du hast mich in eine beßre Welt entrückt. Ich danke dir dafür.

　　還有我最最親愛的家人，媽媽、爸爸還有姊姊，辛苦了。沒有你們我甚至不會是個完整的人。

摘要

在植物面對各式生物性或非生物逆境時、細胞內鈣離子累積為普遍且廣泛的訊息傳遞。在阿拉伯芥有一群包含 34 成員的鈣離子依賴蛋白磷酸激酶家族，同時具有磷酸激酶以及與鈣離子結合的能力，以此參與鈣離子訊息傳遞。其中鈣離子依賴蛋白磷酸激 7 與膜受體感受病原相關分子模式激活的免疫反應(PTI)正調控子 LecRK VI.2 可能有共表現之現象，對於典型 PTI 機制如 MAPK 磷酸化以及癒傷葡聚醣 (callose)累積負調控。更多證據顯示，鈣離子依賴蛋白磷酸激 7 亦參與在荷爾蒙相關的、水楊酸防禦反應、茉莉酸-乙烯防禦反應，例如突變株對於活體營養性病原菌具有抗性但對於死體營養病原菌更感病，荷爾蒙標誌基因分析水楊酸途徑相對應的 *PR1* 有更高的表現，而茉莉酸-乙烯途徑標誌基因 *PDF1.2* 則相對低，顯示了此基因可能會影響兩個重要植物荷爾蒙平衡；另外，PEPR 抗病途徑亦於本基因的突變株當中亦顯示出了更佳之活性。綜合以上所述，在植物抗病反應當中，CPK7 負向調控了 PTI 並且影響 PEPR 抗病途徑與荷爾蒙相關防禦反應。

關鍵字：鈣離子依賴蛋白磷酸激、 細菌性斑點病病原菌、細菌性軟腐病病原菌、灰黴病病原菌、PAMP 誘發免疫反應、水楊酸防禦反應、茉莉酸-乙烯防禦反應、PEPR 抗病途徑。

Abstract

Calcium ions (Ca^{2+}) play an essential and general role as secondary messengers in many cellular signaling pathways. In Arabidopsis, Ca^{2+}-dependent protein kinases (CPKs), a family of 34 members, are able to sense and to response to changes in calcium concentrations through their calcium binding ability and kinase activity. Among these CPKs, CPK7 was selected as a putative co-expressed gene with LecRK-VI.2, a positive regulator of PAMP-triggered Immunity (PTI). In this work, we show that CPK7 negatively regulates typical PTI responses such as callose deposition and MAPK kinase phosphorylation. Concomitantly, knock-out mutant lines of CPK7 were more resistant to the hemibiotrophic pathogen *Pseudomonas syringae* pv. *tomato* DC3000 (*Pst* DC3000). By contrast, *cpk7* mutants were more susceptible to the necrotrophic pathogens *Pectobacterium carotovorum* ssp. *carotovorum* (*Pcc*) and *Botrytis cinerea*. The *cpk7* mutants also demonstrated a potentiated accumulation of *PR1* mRNA upon *Pst* DC3000 infection and less *PDF1.2* up-regulation after *Pcc* inoculation, indicating that CPK7 may also affect hormone responses of plant defense. Furthermore, CPK7 also negatively regulates the (full name needed here) PEPR pathway. These results suggest that in response to calcium signaling triggered by PTI, CPK7 modulates hormone homeostasis and PEPR pathway activity, affecting plant defense to biotic stresses.

Abbreviations

CPK	Calcium-dependent Protein Kinase
PAMPs	Pathogen-associated molecular patterns
PRRs	Pattern-recognition receptors
PTI	PAMPs-triggered immunity
SA	Salicylic acid
JA	Jasmonic acid
ET	Ethylene
DAMP	Danger-Associated Molecular Pattern
DPI	DAMPs-triggered immunity
FRK1	*FLG22-INDUCED RECEPTOR-LIKE 1*
NHL10	*NDR1/HIN1-like 10*
PR1	*PATHOGENESIS-RELATED PROTEIN 1*
PDF1.2	*PLANT DEFENSIN1.2*
PROPEP1	*PRECURSOR OF PEPTIDE 1*
FLS2	*FLAGELLIN-SENSITIVE 2*
BAK1	*BRI1-ASSOCIATED LINASE 1*
BIK1	*BOTRYTIS-INDUCED KINASE1*
PEPR1	*PEP receptor 1*
***Pst* DC3000**	*Pseudomonas syringae* pv. *tomato* DC3000
Pcc	*Pectobacterium carotovorum* ssp. *carotovorum*

Content

Introduction

Pattern-Triggered Immunity

To survive, plants had to adapt to be able to resist to numerous stresses from the harsh environment they are living in. To resist biotic stresses such as bacterial or fungal pathogens attack, plants has developed several adaptive mechanisms (Van Verk et al., 2009). Among these molecular defense mechanisms, the very first one during plant-pathogen interaction is plant innate immunity. Like those of animal immune systems, plant innate immunity is defined as recognition and reaction to pathogenic or non-pathogenic microbes (Boller, 2009). In more details, when microbes approach a plant cell, some molecular patterns such as flagellin and elongation factor Tu are passively released. These microbial signatures, termed pathogen-associated molecular patterns (PAMPs), are then captured and recognized by plant protein receptors localized on the surface of plant cells. Recognition will lead to the activation of downstream defence signaling events (Jones and Dangl, 2006). Plant receptor proteins are termed pattern-recognition receptors (PRRs) and the whole pattern-recognition phenomenon is further defined as pattern triggered immunity (PTI) (Ausubel, 2005; Boller and Felix, 2009).

PTI events include accumulation of reactive oxygen species (ROS), stomatal closure and callose deposition (Boller and Felix, 2009). These defense responses either create chemical stresses or physical barriers, enabling host to successfully generate a
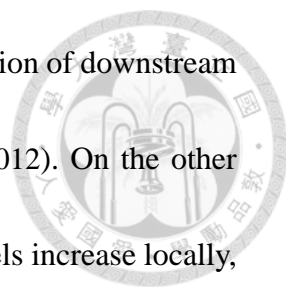
basal resistance against invading pathogens such as hemibiotrophic bacterial pathogen *Pseudomonas syringae* pv. *tomato* (*Pst*) and necrotrophic *Pectobacterium carotovorum ssp. carotovorum* (*Pcc*) (Singh et al., 2012). Furthermore, PTI is also accompanied with an intensive transcriptional change. Former studies have found two pathways mediating near membrane signals and transcriptome. First, mitogen-activated protein kinase (MAPK) cascade, which takes advantage on phosphate groups transferring through proteins with different energy levels (Dong et al., 2002). The other one is ion influx (Boudsocq et al., 2010), such as calcium oscillation, created by membrane-localized calcium channel, sensed by cytosolic calcium sensing proteins, such as calcium dependent protein kinases (CPKs) (DeFalco et al., 2010; Sanders et al., 2002). PTI-responsive genes such as *FRK1* and *NHL10* will be up-regulated, depending on these underlying signal transductions after PRRs recognition of PAMPs (Zipfel et al. 2004).

In *Arabidopsis thaliana*, a well-studied model for PTI includes the PRR FLAGELLIN-SENSITIVE 2 (FLS2) and the co-receptor BRI1-ASSOCIATED RECEPTOR KINASE 1 (BAK1). In this model, the PRR FLS2 perceives PAMPs such as bacterial flagellin fragments and then associates with BAK1, another membrane LRR-PK, then with cytosolic cofactor such as BRASSINOSTEROID INSENSITIVE1 (BIK1), this kinase complex is able to amplify the PTI signals and triggers downstream PTI responses (Gomez-Gomez, 2001; Chinchilla et al., 2009). However, besides FLS2

and BAK1, in a previous study, the Zimmerli laboratory discovered the Lectin Receptor Kinase-VI.2 (LecRK-VI.2), which serves as a positive regulator of PTI (Singh et al., 2012). Over-expression lines of LecRK-VI.2 show constitutive PTI gene activation and callose deposition with higher resistance to pathogen in comparison to wild-type. These evidences suggest that in addition of the recognition ofPAMPs by PRRs, there should be more players with more different kinds of patterns, involved in the PTI response.
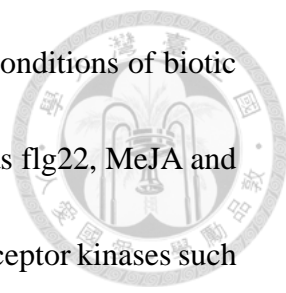
SA-, JA/ET-dependent defense and PEPR pathway

Given the fact that the infection of pathogen occurs during a long period of time, on several tissues and with multiple infectious strategies, a great challenge to plants is to maintain the energy homeostasis during activating defense responses (Glazebrook, 2005; Pieterse et al., 2009). With this aspect, signaling crosstalk between major defense-related hormones is necessary. Current thinking is that salicylic Acid (SA) induces resistance against biotrophic pathogens due to programmed cell death in the host (Pieterse et al., 2009). However, since necrotrophic pathogens even benefit from host cell death, defense responses requiring jasmonic acid (JA) and ethylene (ET) signaling will be activated in this situation (Bari and Jones, 2009). For SA-dependent signaling pathway, in response to pathogen attack, SA INDUCTION DEFICIENT 2 (SID2) and PHYTOALEXIN DEFICIENT 4 (PAD4) act upstream of SA to promote SA accumulation (Feys et al., 2001). These SA signals will be perceived by the SA receptor

NON-EXPRESSOR OF PR1 (NPR1) to further promote the expression of downstream

associated genes such as *PR1* and other *R*-genes (Pieterse et al., 2012). On the other

hand, after detecting pathogen infections and tissue damage, JA levels increase locally,

and its chemical derivate JA-Isoleucine (JA-Ile) is recognized by CORONATINE

INSENSITIVE1 (COI1), enhancing the expression of *PLANT DEFENSIN1.2* (*PDF1.2*).

(rewrite this sentence as it is not possible to understand what you want to say here…),

suggesting that JA and ET contribute simultaneously to this pathway (Feys et al., 1994;

Yan et al., 2009).
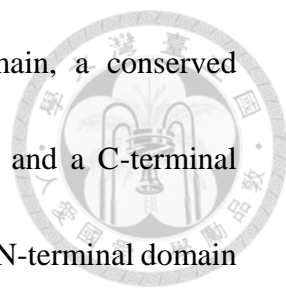
Based on several pathological and molecular evidences, SA and JA/ET signaling

pathways are believed to be antagonistic (de Torres et al., 2009). For example, *mpk4*

mutant has strong deficiency of *PDF1.2* expression while having constitutive activation

of SA-dependent pathway (Peterson, 2000). However, several studies suggest that the

regulation between these two pathways is actually more complex than just simply

antagonistic. In leaves of (abbreviation defined before?)WT Arabidopsis applied with

Arabidopsis danger peptides (AtPeps), both transcriptional levels of *PR1* and *PDF1.2*

will be induced. This evidence suggests the existence of at least one circumstance when

SA-dependent and JA/ET dependent pathway can be equally activated (Ross et al.,

2014). Recently, more information about these endogenous peptides and their functions

in plant defense were revealed. Similar as many other endogenous danger-associated
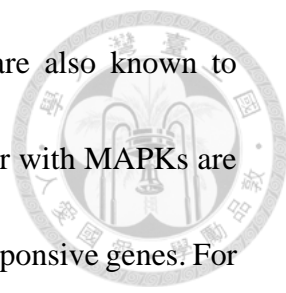
molecular patterns (DAMPs), AtPeps are passively induced under conditions of biotic stress, such as microbial infections, the detection of MAMPs such as flg22, MeJA and ET treatment, then recognized by some leucine-rich repeat (LRR) receptor kinases such as Pep Receptors (PEPRs), to initiate intracellular signaling and later activating the defense responsible genes and expression of propeptides themselves (Yamaguchi et al., 2010; Huffaker and Ryan, 2007). This mechanism is defined as the PEPR pathway. The PEPR pathway mainly leads to two different categories of defense systems. The application of AtPEPs triggers PTI-like responses, such as callose deposition and ion influx (Bartels et al., 2013). Moreover, application of AtPeps will cause the accumulation of JA and induce both SA-dependent and JA/ET dependent pathway and consequently enhances plant resistance to pathogen (Ross et al., 2014).

CPKs and CPK7

In plant, calcium is a ubiquitous second messenger,that mediates many different environmental stress responses (Boudsocq et al., 2010). In normal condition, calcium is maintained in the cytosol at very low level (100-200 nM) and accumulates in a very high level during stimulation (Downie, 2014). To decipher the amplitude, duration and frequency of cytosolic calcium oscillation created by different stresses, calcium sensors, such as calcium-dependent protein kinases (CPKs) are able to react in response to calcium concentration by direct binding to calcium ion (Romeis and Herde, 2014). The

basic structure of CPKs consists of a variable N-terminal domain, a conserved

serine/threonine kinase domain, an autoinhibitory junction region and a C-terminal

regulatory CaM-like domain (CamLD) (Christodoulou et al., 2004). N-terminal domain

often contains predicted acylation sites, and autoinhibition inactivates kinase activity

by a pseudosubstrate association. The CamLD domain contains four EF-hand calcium

binding motifs. Recent study on protein structure demonstrates the activation of CPKs.

In normal condition, autoinhibition domain attaches to the kinase activation site as a

pseudosubstrate thus inactivated the kinase. Upon rising Ca^{2+} level, autoinhibition

region releases from kinase active site through conformational change by Ca^{2+} binding

(Christodoulou et al., 2004; Weljie and Vogel, 2004). In Arabidopsis, CPKs consists of

a large family of 34 genes and are divided into four groups (Fig. 1) (Boudsocq and

Sheen, 2013; Chen, et al., 2002). Many of the members from the CPK family have

already been identified to be involved in biotic stress signaling pathways, either with

stimulus-dependent biochemical reactions on transcriptome alternation or alternation

of cellular phosphorylation pattern (Boudsocq and Sheen, 2013). For example,

overexpression of *CPK1* induces a broad-spectrum Arabidopsis resistance to bacteria

and fungi by triggering SA accumulation through the induction of SA regulatory and

biosynthesis genes such as *PAD4* and *SID2* (Coca, 2010). And for Ca^{2+} spiking upon

herbivore attack *AtCPK3* and *AtCPK13* serve as positive regulators of *PDF1.2*

induction upon caterpillars attack (Kanchiswamy, 2010). CPKs are also known to function in PTI signaling (Gao et al., 2014). Notably, CPKs together with MAPKs are critical for the activation of targeted transcription factors and PTI-responsive genes. For instance, *AtCPK4*, *AtCPK5*, *AtCPK6* and *AtCPK11* positively regulate *NHL10* synergistically with MAPK cascade upon flg22 treatment (reviewed by Boudsocq and Sheen, 2013).

Members of Zimmerli laboratory have identified several genes that are putatively co-expressed with the positive regulator of the PTI response LecRK-VI.2. Among them (Table S1), CPK7 was selected for further research. Some *in vitro* biochemical assays have already been performed on CPK7. With these evidences, CPK7 is proposed to be an active kinase and is capable of Ca^{2+} binding. However its kinase activity is independent of calcium concentration (Boudsocq, 2012). Further studies with a T-DNA insertion CPK7 knock-out indicates that CPK7 negatively regulates aquaporin activity by repressing cellular PIP2 expression levels in root (Li et al., 2014). In addition, CPK7 along with BIK1 is reported to be phosphorylated by flg22 treatment *in vivo* (Li et al., 2015). Here, by applying reverse-genetic approach with two knockout mutant lines termed *cpk7* 36-1 and *cpk7* 36-2, we suggest that CPK7 acts downstream of PTI, modulating SA-dependent, JA/ET dependent plant defense and PEPR pathway, but the certain role of how CPK7 plays, is remain unclear.

Material and Methods

Plant Materials and Growth Conditions

Arabidopsis ecotype Col-0 plants were grown in commercial potting soil/perlite (3:2) at 22℃ to 24℃ day and 17℃ to 19℃ night temperature under a short day (9-h-light/15-h-dark) photoperiod. The lighting is supplied at an intensity of ~100 µE m^{-2}s^{-1} by fluorescence tubes. T-DNA insertion mutant *cpk7* 36-1 (SALK_035601) and *cpk7* 36-2 (SALK_127223) were obtained from the Arabidopsis Biological Resource Center (ABRC). Bacterial Pathogens *Pst* DC3000 and *Pcc* were cultivate at 28℃ and 220 rpm in King's B medium containing 50mg/mL rifampicin or 100 mg/mL ampicillin, respectively. The fungus *B. cinerea* was grown at room temperature (18℃ ~ 25℃) with high humidity on PDB-agar plates for 2 to 3 weeks as described (Zimmerli et al., 2001).

Pathogen Infection Assay

For bacterial pathogen, five-week-old Arabidopsis plants were dipped in a bacterial suspension of 2 x 10^7 colony-forming units (CFU)/mL *Pst* DC3000 or 10^6 CFU/mL *Pcc* in 10 mM MgSO4 containing 0.01% Silwet L-77 (Lehle Seeds) for 15 min. After dipping, plants were kept at 100% relative humidity overnight. Disease symptoms were evaluated at 3 days post inoculation (dpi). For bacterial titers, leaf discs

collected at 2 dpi were washed twice with sterile water and homogenized in 10 mM

MgSO4. Quantification was done by plating appropriate dilutions on King's B agar

containing rifampicin (50mg/liter) as previously described (Zimmerli et al., 2000).

Each biological repeat represents nine leaf discs (0.5 cm diameter) from three different

plants.

For fungal pathogen infection, spores of *B. cinerea* were suspended in PDB at a

final concentration of 10^5 spores/mL. Eight μL droplets of inoculum were deposited on

4 leaves of 5-week-old plants (8 plants for each genotypes). Pictures of lesions were

captured 2 to 3 days after inoculation, and lesion perimeters were evaluated by using

the ImageJ software (http://rsb.info.nih.gov/ij/).

Oxidative Burst Kinetic Assay

Reactive Oxygen Species (ROS) evaluation was performed as previously

described (Keppler et al., 1989). Eight leaf discs of 0.25 cm^2 from three 5-week-old

Arabidopsis plants were incubated in 100 μL ddH$_2$O for 16 h in 96-well plates. Water

was then replaced by 100 μL of reaction solution containing 50 μM of luminol and 10

μg/mL of horseradish peroxidase (Sigma) supplemented with 10 nM of flg22 or water

only for the mock controls. ROS measurements expressed as means of RLU (Relative

Light Units) were measured immediately after adding the solution with a Centro

LIApcLB 692 plate luminometer (Berthold Technologies, Bad Wildbad, Germany).

ROS evaluation was performed at 2 min interval reading times for a period of 34 min.
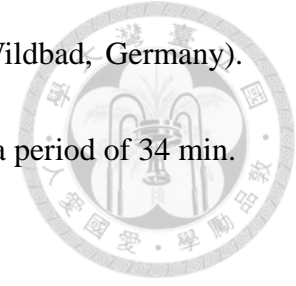
Stomatal Assay

Plants were kept under light for at least 3 h to open stomata. Leaf peels were

collected from the abaxial side of fully expanded leaves and floated in stomatal buffer

(10 mM MES-KOH, 30 mM KCl, pH 6.15) for 2.5 h under light ($\sim$100 μE m^{-2} s^{-1}).

After treatment with mock control (10 mM MgSO4) or 10^8 CFU/mL *Pst* DC3000 in 10

mM MgSO$_4$, pictures of stomata were taken of random regions at various time points

using an Olympus BX51 microscope digital camera and application software DP2-

BSW. Stomatal apertures were measured using the "measure" function of ImageJ

(http://rsb.info.nih.gov/ij/). Three plants were used per biological replicates.

Callose Staining Assay

Leaves of 5-week-old Arabidopsis were syringe infiltrated 500 nM flg22 dissolved

in H$_2$O. Control, mock-treated plants were infiltrated with H$_2$O only. Twelve leaf discs

from three different plants were selected for analyses. Harvested leaf samples were

cleared overnight by incubation in 95% ethanol at room temperature and then washed

three times (0.5 h for each time) with sterilized H_2O. Transparent leaves were stained

with 0.01% aniline blue in 0.15 M phosphate buffer, pH 8, for 1 h. Callose deposits

were visualized under UV illumination using an Olympus BX51 micro-scope digital

camera and application software DP2-BSW. Callose deposition was evaluated using the

"analyze particles" function of ImageJ (http://rsb.info.nih.gov/ij/).

MAPK Phosphorylation Assay

Nine leaves of 5-week-old Arabidopsis were syringe infiltrated with 100 nM flg22

dissolved in H_2O. Control plants were infiltrated with H_2O only. Samples were

collected after 10 min and immediately snap frozen in liquid nitrogen. The protein

concentration was determined using the BCA protein assay kit (Bio-red) with BSA as

a standard. Protein crude extracts were separated on 10% SDS gel, and proteins were

transferred to Polyvinylidene fluoride membrane (PVDF) by immunoblotting (Mini-

Protean II system; Bio-Rad). Activated MAPK3/MAPK6 were detected by overnight

incubation with anti-p42/44 MPK primary antibodies (1:3000 dilution, Cell Signaling

Technology), followed by incubation with anti-rabbit-HRP secondary antibodies (Sig-

ma-Aldrich) for 1 h. The signals were visualized using an enhanced chemiluminescence

system (Western Lightning Plus-ECL kit; Perkin-Elmer) following the manufacturer's

instructions and LAS-3000 (Fujifilm).

PAMP Treatment

For determining *FRK1* and *NHL10* response to PAMPs, leaves of 5-week-old Arabidopsis were syringe-infiltrated with 100 nM flg22 dissolved in H_2O or ddH_2O as Mock control. Samples were collected at 5 h post infiltration. For *PR1* expression analysis, leaves were syringe-infiltrated with 10^8 CFU/mL *Pst* DC3000 or ddH_2O only as Mock control. Infiltrated leaves were collected at 5 h and 9 h post inoculation. For *PDF1.2* expression, leaves were syringe-infiltrated with *Pcc* 5 x 10^6 CFU/mL or sprayed with spores from *B. cinerea* at a concentration of 10^5 spores/mL in PDB. Infiltration of ddH2O or spraying with PDB was used as mock control respectively. Plants were kept in high humidity sealed boxes for 24 h before samples collection. For *FRK1* and *PROPEP1* expression, 10 of 10-day-old seedlings were growth on ½ MS agar plates, and then moved to 6-well plate where each well contains ½ MS 6 mL for recovering from possible wounding effect overnight, then for the experiment, directly add additional pep1 to 50 nM each well and collect samples snap frozen in liquid nitrogen every 1 h until 6 h.

RNA Extraction and qRT-PCR

Total RNA was extracted and purified using the MaestroZol reagent according to the manufacturer's instructions (Omics Biotechnology Co., Ltd) with the addition of PLUS reagent for polysaccharides and proteoglycans elimination. Genomic DNA contaminations were removed using Qiagen RNase-Free DNase Set. For cDNA synthesis, 2 μg of total RNA were prepared in a volume of 22 μL DEPC-treated H_2O and denatured at 65°C for 5 min. Eighteen point five mL of master mix (16 μL of M-MLV buffer, 1 μL of 10 mM dNTP, 1 μL of 100 mM OligoT, 0.5 μL of 100 U M-MLV reverse transcriptase, [Invi-trogen]) was added into each tube and then incubated at 37°C for 1 h, and 70°C for 10 min. The cDNA was then diluted 5-times before quantitative RT-PCR (qRT-PCR) analyses. The cycling conditions were 94°C for 3 min for one initial step followed by 94°C for 30 s, 58°C for 30 s, and 72°C for 1 min, for 35 cycles. The PCR was terminated with one extra step at 72°C for 10 min. qRT-PCRs were conducted on a CFX Real-Time PCR Detection System (Bio-Rad). SYBR Green fast qPCR master mix (Bio-Rad; 1 μL of cDNA, 5 μL SYBR Green supermix, 5 μL filtered sterile H_2O, 0.5 μL of 10 mM forward and reverse primers, in a total volume of 12 μL per well) was employed for the analysis. The cycling conditions were composed of an initial 3 min denaturation step at 95°C, followed by 40 cycles at 95°C for 3 s and 60°C for 30 s. Melting curves were run from 65°C to 95°C with 0.5-s time

interval to ensure the specificity of product. Data were analyzed using Bio-Rad CFX

manager software. *UBQ10* was used as a reference gene for normalization of gene

expression levels in all samples. The wild-type (WT) without any treatment or mock

treatment were considered as controls in each experiment. All primers used for qRT-

PCR amplification are listed in supplemental table S1.

Subcellular Localization

The full-length *CPK7* cDNA was PCR amplified from wide type Col-0 cDNAs

using the primers listed in Table S2, The PCR product was cloned into

pCR8/GW/TOPO vector (Invitrogen). The TOPO vector with full length genomic

LRR50 was then sequenced to ensure fidelity (Tri-I Biotech). After confirmation by

sequencing, TOPO-LRR50 was recombined into the Gateway-compatible destination

vector pEarlyGate 103 (obtained from ABRC) containing the 35S promoter and GFP-

6x His tag through LR reaction according to the manufacturer's instructions

(Invitrogen). The recombination plasmid after the LR reaction was transformed into *E.

coli* strain DH5α competent cells (Omics Bio). The DH5α competent cells were then

incubated at 37℃ on LB agar plate with 100 ng/mL Kanamycin for selection. Colony

PCR was performed to screen for positive colonies using the forward primer 5'-

AAGGGTCTTGCGAAGGATAG -3' from the 35S promoter region and the reverse

primer 5'- CCGAGCCGTTGGGCTCAGT -3' from the LRR50 region. The positive *E. coli* colonies were picked up and grown overnight in LB medium containing 100 ng/mL kanamycin at 37˚C. The plasmids DNA were extracted by plasmid Mini kit (GeneMark). Arabidopsis protoplasts were isolated and transfected by a polyethylene glycol method as described previously (Yoo et al., 2007). Briefly, 0.1 mL of protoplast suspension (200,000 cells mL^{-1}) was transfected with a mixture of 4 μg of plasmid. After transfection, protoplasts were incubated 16 h, and then samples were visualized using a TCS SP5 confocal spectral microscope imaging system (Leica)

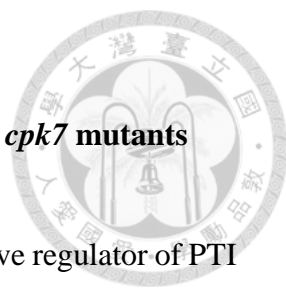**Bimolecular Fluorescence Complementation Assay in Arabidopsis Protoplast**

For Bimolecular Fluorescence Complementation (BiFC) assay, plasmids containing *CPK7*-YN, *PEPR1*-YN, YC-*CPK7*, YC-*PEPR1* were constructed. *PEPR1* CDS was PCR amplified from wide type Col-0 cDNA using the primers listed in Table 1 (name needed) and PCR products were then cloned into the pCR8 TOPO vector. TOPO-cDNA plasmids were finally recombined into the Gateway-compatible expression vectors pSAT4 (A)-DEST-n (1-174) EYFP-N1 (pE3134) (obtained from Stanton B. Gelvin's lab, Purdue University). Plasmids of CPK7-YN, CPK7-YC, FLS2-YC, BAK1-YC, BAK1-Yn, BIK1-YC, PEPR1-YC or PEPR1-YN with different combinations were transformed into Arabidopsis protoplasts by polyethylene glycol for

transient expression (Yoo et al., 2007). After 16 h incubation, samples were visualized

using a TCS SP5 confocal spectral microscope imaging system (Leica).
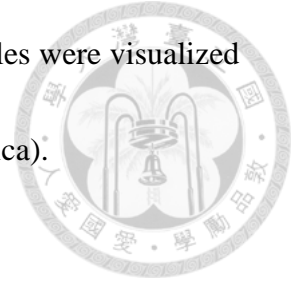
Results

**Enhanced resistance to hemi-biotrophic bacteria in Arabidopsis *cpk7* mutants**

To evaluate whether *CPK7*, a gene co-expressed with the positive regulator of PTI *LecRK VI.2*, the resistance response of *cpk7* mutants to hemi-biotrophic bacteria was evaluated. In comparison with WT Col-0, on the third day after challenged with *Pst* DC3000, two *cpk7* mutant alleles developed less necroses and bacteria-mediated leaf yellowing (Fig. 3a). Similarly, bacterial titers were significantly lower in *cpk7* mutants than in Col-0 (Fig. 3b), suggesting that CPK7 acts as a negative regulator of Arabidopsis defense to hemi-biotrophic pathogens such as *Pst* DC3000.

The *cpk7* mutants generate WT-level of reactive oxygen species burst upon flg22 perception

To further evaluate the role of CPK7 in Arabidopsis defense, we tested PTI-mediated ROS production in both *cpk7* alleles. The oxidative burst is indeed considered as a common PTI response that is rapidly induced after PAMP treatment and creates a chemical stress to pathogen (Boller and Felix, 2009). ROS production of leaf discs from WT and *cpk7* mutants after treatment with 100 nM flg22 was evaluated by detecting hydrogen peroxide (H_2O_2)-dependent luminescence of luminol. Within 34 min, *cpk7*

mutants have the same ROS productivity as WT, both in amplitude and sensitivity (Fig. 4). These data suggest that CPK7 does not play a role in the PTI-mediated ROS burst.
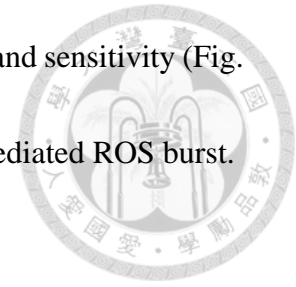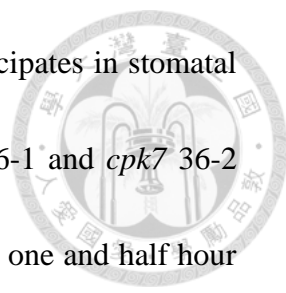
CPK7 negatively modulates PTI-mediated callose deposition

Callose is a polysaccharide in the form of β-1, 3-glucan and accumulates on the cell wall of plants leading to mechanical reinforcement against pathogens invasion (Chen and Kim, 2009). Since PAMP treatment causes callose accumulation in plant tissues, callose deposition is thought be a biological signature of PTI activation (Boller and Felix, 2009). After 100 nM flg22 infiltrations, leaves of both *cpk7* mutant alleles produced significantly more callose deposits at 6 h and 9 h post infiltration when analyzed by the aniline blue staining method (Fig. 5a -5d). These results suggest that CPK7 acts as a negative regulator of PTI-mediated callose deposition.

CPK7 is not critical for stomatal innate immunity

Stomatal movement is controlled by multiple factors such as circadian clock, evapotranspiration and also critical for plant-microbe interaction (Misra et al., 2015). During bacterial pathogen infection, guard cells close to form a physical barrier blocking invading entrance (Melotto et al., 2006). This procedure is regarded as a part

of the plant innate immunity response. To test whether CPK7 participates in stomatal immunity, stomatal apertures in epidermal peels of Col-0, *cpk7* 36-1 and *cpk7* 36-2 were measured upon *Pst* DC3000 inoculation. In normal condition, one and half hour after *Pst* DC3000 infection, stomata close for limiting bacteria entry. However, the virulent *Pst* DC3000 secretes the virulence factor coronatine (COR) to actively reopen stomata at 3 hpi. In epidermis peels of the two *cpk7* mutants, WT stomatal closure was observed after *Pst* DC3000 inoculation (Fig. 6). Hence, *CPK7* may not play a critical role in Arabidopsis stomatal innate immunity.

Higher MPK3/MPK6 phosphorylation level is observed in *cpk7* mutants after flg22 treatment

Downstream of PRRs-mediated recognition of PAMPs, a complete MAPK cascade including MEKK1-MKK4/5-MPK3/6 transfer PTI signaling through a serie of transphosphorylation events (Asai et al., 2002). Hence, phosphorylation of MPK3/MPK6 is regarded as a maker for PTI activation. To determine whether *CPK7* affects the MAPK cascade, leaves of Col-0, *cpk7* 36-1 and *cpk7* 36-2 mutants were infiltrated with 1 μm flg22. MPK3/MPK6 phosphorylation levels were higher in the *cpk7* mutants than in Col-0 WT (Fig. 7), indicating that MAPK cascade is more active

26

in the absence of CPK7. Hence, CPK7 may negatively regulate the PAMP-mediated
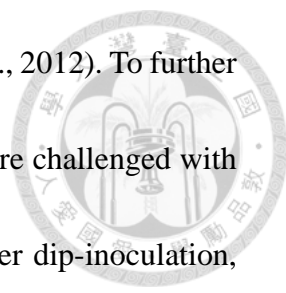
MAPK cascade.

PTI marker genes up-regulation is comparable between WT and *cpk7* mutants

As well as other defense mechanisms, activation of PTI is accompanied by

tremendous transcriptional alterations (Zipfel et al., 2004). Since *cpk7* mutants appear

to have a stronger activation of MPK3/MPK6, we hypothesized that PTI maker genes

downstream of the MAPK cascade should be up-regulated. To test this hypothesis, 500

nM of flg22 were infiltrated into leaves of Col-0, *cpk7* 36-1 and *cpk7* 36-2, and the

expression levels of the PTI marker genes *FRK1* and *NHL10* were evaluated at 5 h after

infiltration. Surprisingly, up-regulation of both *FRK1* and *NHL10* was at WT levels in

the *cpk7* mutants (Fig 8a and b). This result indicates that, although MPK3/MPK6 is

more activated in *cpk7* mutants, the transcriptional level of downstream *FRK1* and

NHL10 may not be affected, at least in the condition tested in our experiment.

cpk7* mutants demonstrate a susceptible phenotype to necrotrophic *Pcc* and *B.

***cinerea* infections**

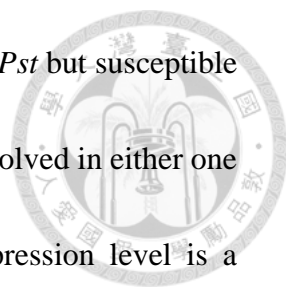Overexpression of *LecRK VI.2* in Arabidopsis enhances resistance to both

biotrophic *Pst* DC3000 and necrotrophic *Pcc* pathogens, (Singh et al., 2012). To further

investigate the function of CPK7 in plant defense, *cpk7* mutants were challenged with

necrotrophic *Pcc* bacteria. Observing symptoms on the 2nd day after dip-inoculation,

more bacteria-mediated lesions were produced on leaf areas of *cpk7* 36-1 and *cpk7* 36-

2 then on Col-0 WT (Fig. 9a). By measuring bacterial titers, similar with symptom

observation, both *cpk7* mutant alleles were significantly more susceptible to *Pcc* than

to Col-0 WT (Fig. 9b). These results suggest that *CPK7* may positively regulate the

Arabidopsis defense responses to *Pcc*.

To determine whether the susceptibility in *cpk7* mutants is due to necrotrophic

nutrition, we then performed disease assay with *B. cinerea*, a necrotrophic fungi. After

3.5 days from inoculation, lesion circles on *cpk7* 36-1 and *cpk7* 36-2 were larger than

those on Col-0 (Fig. 10a). This result was also quantified by measuring lesion perimeter,

also showed that the symptom of *cpk7* mutants is much more severe than Col-0 (Fig

10b). Together these observations indicate that mutations in CPK7 cause a loss of

resistance to necrotrophic pathogen.

Expression of *PR1* is potentiated in *cpk7* mutants

Plants take advantage of SA-dependent defense upon biotrophic pathogen attack

and JA/ET-dependent defense for necrotrophic pathway (Pieterse et al., 2009; Bari and

Jones, 2009). Since *cpk7* mutants were resistant to hemi-biotrophic *Pst* but susceptible

to necrotrophic pathogens, we hypothesized that *CPK7* could be involved in either one

of the two hormone-related defenses. Determination of *PR1* expression level is a

common method to evaluate the activation of the SA-dependent pathway (Bari and

Jones, 2009). Leaves of Col-0, *cpk7* 36-1 and *cpk7* 36-2 were syringe-infiltrated with

10^7 cfu/mL of *Pst* DC3000, after 5 h, *PR1* expression in *cpk7* 36-1 and *cpk7* 36-2 was

more up-regulated then in Col-0 WT (Fig. 11a), in which up-regulation only started at

9 hpi when in *cpk7* mutants, *PR1* expression levels were already decreased (Fig. 11b).

Consequently, by monitoring expression of *PR1*, we suggest that SA-dependent

pathway in *cpk7* mutants is more active.

cpk7 mutants accumulate less *PDF1.2* transcripts upon Pcc infiltration but

normal level upon B. cinerea infection

Like *PR1* for SA-dependent defense, *PDF1.2* serves as the marker gene for JA/ET-

dependent pathway (de Torres et al., 2009). Leaves of Col-0, *cpk7* 36-1 and *cpk7* 36-2

were syringe-infiltrated with 10^6 cfu/mL of *Pcc*. After 1 day, up-regulation of *PDF1.2*

in *cpk7* 36-1 and *cpk7* 36-2 was weaker than in Col-0 WT (Fig. 12a). For measuring

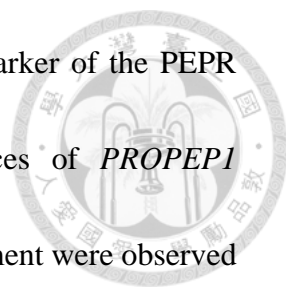*PDF1.2* expression upon *B. cinerea* infection, Col-0 and *cpk7* mutants were uniformly

sprayed with 5 x 10^6 spores/mL from *B. cinerea*. Surprisingly, after 1 day, *PDF1.2* is fully up-regulated and the expression levels are similar between Col-0 and the two *cpk7* mutants (Fig. 12b), indicating that there exists at least one circumstance in which *cpk7* mutants is able to activate WT levels of the JA/ET responses. Results of these experiments on hormone-related defenses suggest that *CPK7* might be required for signal crosstalk between SA-dependent and JA/ET- dependent pathways.

CPK7 negatively regulates *FRK1* expression upon pep1 treatment but not *PROPEP1* expression

Recently, PEPR pathway was shown to act downstream of PTI and to regulate hormone related-defenses (Ross et al., 2014). Activation of PEPR pathway is accompanied with *FRK1* up-regulation. To determine whether CPK7 take parts in the PEPR signaling pathway, *FRK1* expression levels after 50 nM pep1 treatment was monitored for 6 hours. Interestingly, expression of *FRK1* in Col-0 was low and rapidly decreased at 4 h. Meanwhile in the two *cpk7* mutants, *FRK1* expression was higher and did not decrease until 5 h (Fig. 13a). This prolonged signal implies that CPK7 might serve as a negative regulator of the PEPR pathway.

Besides *FRK1*, it is also known that PEPR pathway forms a positive loop itself, so

induction of transcriptional expression of *PROPEP*s is another marker of the PEPR

pathway (Huffaker and Ryan, 2007)). No significant differences of *PROPEP1*

expression levels between Col-0 and *cpk7* mutants upon pep1 treatment were observed

(Fig. 13b), suggesting that the amplification of *FRK1* in *cpk7* 36-1 and *cpk7* 36-2 is not

a consequence of intrinsic pep1 production.

CPK7 is localized on the plasma membrane and nucleus and localization is

affected by flg22 treatment

To further investigate the characteristic of CPK7, subcellular localization of

CPK7 was analyzed by transient assay system with GFP fused proteins. Interestingly,

the fluorescence signals could be detected in nucleus and on membrane

simultaneously but not in cytosol (Fig. 14). Nonetheless, addition of flg22 arouse

changes to localization of CPK7, after treatment, fluorescence signals on membrane

were stronger while weaker in nucleus. This result in advanced suggests that CPK7

participates in the downstream of PTI.

CPK7 does not associate with FLS2, BAK1, BIK1 and PEPR1

This work proposes several evidences linking CPK7 to the PTI response, further

influencing hormone-related defenses and the PEPR pathway. FLS2, BAK1 and BIK1

act as core proteins of one of the PRR involved in PTI (Chinchilla, 2007). On the other

hand, PEPR1 is the receptor for pep1, therefore is critical for the PEPR pathway

(Yamaguchi et al., 2010). We thus used the BiFC assay to determine whether CPK7

associates with these proteins. None of these well-studied components of PTI (Fig. 15a)

or PEPR pathway (Fig. 15b) associated with CPK7, indicating that there must be other

way for CPK7 to influence plant defenses.
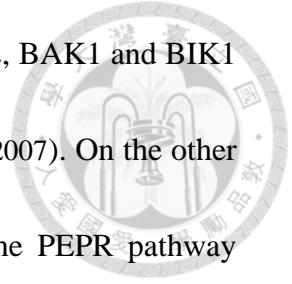
Discussion

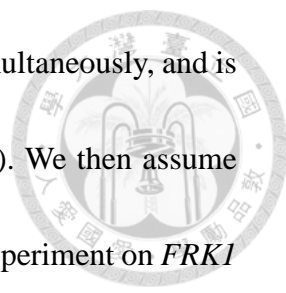**CPK7 plays a role in the Arabidopsis PTI as a negative regulator.**

In accordance of being activated by stresses triggering Ca^{2+} oscillation, members in CPK family are often thought to play a positive role upon stresses (Boudsocq and Sheen, 2013). Recently, study on CPK28 clearly demonstrated that CPK28 actively suppresses PTI responses by directly phosphorylating RBOHD (Monaghan et al., 2015). This report reveals a new characteristic of CPKs, CPKs can indeed also act as a negative regulator to certain stress responses. Here, we find a novel negative regulator of PTI from the CPK family, CPK7. *cpk7* mutants were more resistant to hemi-biotrophic bacterial pathogen, *Pst* DC3000, and were more active on MAPK phosphorylation and callose deposition, suggesting a negative effect of CPK7 to plant innate immunity. In comparison with CPK28, which is shown to rapidly repress the PTI response, notably the oxidative burst, the regulatory function carried by CPK7 is rather at a later stage of the PTI response, such as callose deposition. Confusingly, although activities of MPK3/MPK6 were inhibited by CPK7, gene expression of downstream gene *FRK1* and *NHL10* were not increased under our condition. Possible explanation to this contradiction is, first, methodologically, we did miss the proper time point at which expression levels of mutants and Col-0 differentiated. In other words, the effect from the absence of CPK7 is covered by other mechanism.

CPK7 modulates SA-dependent and JA/SA-dependent defense and CPK7

negatively regulates PEPR pathway.

Typical PTI responses conduct a wide-range of resistance to both necrotrophic and biotrophic pathogens (Singh et al., 2012). However, our results show that *cpk7* mutants are more susceptible to necrotrophic pathogens. Research on SA-dependent defense indicates that, during biotrophic pathogen attack, SA quickly accumulates in local invading region, triggering programmed cell death, and soon being transported to protect adjacent cells (Greenberg and Yao, 2004). Consistent with this information, *PR1* expression in *cpk7* mutants is earlier induced and decreased, inferring a sensitive SA-dependent pathway. On the other hand, our results show that *PDF1.2* expression is impaired after *Pcc* treatment but not after *B. cinerea* in *cpk7* mutants. In comparison with SA, JA/ET-dependent pathway underlies several feed-back loops and seems to be more complex (Bostock, 2005), several hypothesizes could be provided. Perhaps from the beginning, PAMPs from bacteria or from fungus have different effects of CPK7, leading to the different pattern of JA/ET regulation. Based on these evidences, the regulatory mechanism of CPK7 to hormone-related defense network is much more likely to be temporary and buffering rather than constitutive. Confronted with the traditional mutual antagonism between SA and JA/ET (de Torres et al., 2009), PEPR

pathway activates SA-dependent and JA/ET-dependent defenses simultaneously, and is also regulated by PTI (Ross, et al., 2014; Huffaker and Ryan, 2007). We then assume that CPK7 regulates SA-JA/ET crosstalk through PEPR pathway. Experiment on *FRK1* and *PROPEP1* upon pep1 treatment suggest that CPK7 negatively regulator to PEPR pathway but not due to up regulation of *PROPEP1* expression. Yet hardly could we deduce to our hypothesis that CPK7 acts upstream of PEPR pathway to regulate SA-JA/ET, more evidences are needed. Finally, note that the induced resistance to *Pst* DC3000 and susceptibility to *Pcc* and *B. cinerea* are in *cpk7* mutants are consist with those of *ein2* knock-out plant (Thomma et al., 1998), with the same phenotype as *cpk7* mutants, giving us a clue that CPK7 might also involve in ethylene signaling pathway. A pilot exam of *ERF1* expression upon ACC treatment was performed showing deficiency on two *cpk7* mutants (see Fig. S2).
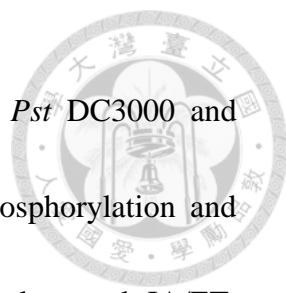
CPK7 acts downstream of PTI, modulating several defense pathways

Since no clear association between CPK7 and the core components of PTI and PEPR pathway could be observed, the direct function of CPK7 still remains unknown. A HPLC-MASS analysis on *cpk7* mutants has already be done (Li et al., 2014). However, without any elicitor treatment, no well-known defense-related genes could be identified. Thus for surveying over possible interactome of CPK7, and again, with

the fact that CPK7 is a constitutive active kinase which localized on nucleus and membrane, phosphoproteomic-based screening and with PAMP treatment might be a feasible way. In conclusion, on the basis of our results, CPK7 acts downstream of PTI, negatively regulate SA-dependent and PEPR pathway, but might be critical for full activation of the JA/ET pathway.
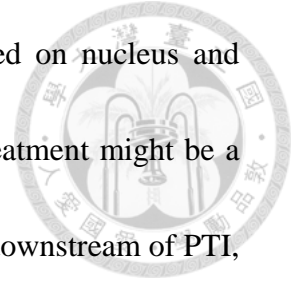
Conclusion and future perspectives

CPK7 serves as a negative regulator of plant resistance to *Pst* DC3000 and suppresses some of the PTI responses such as MPK3/MPK6 phosphorylation and callose deposition. Nonetheless, CPK7 also modulates SA-dependent and JA/ET-dependent pathways by fast accumulation of *PR1* mRNAs and less *PDF1.2* up-regulation upon bacterial pathogen attack and thus having a susceptible phenotype to necrotrophic pathogens such as *Pcc* and *B. cinerea*. CPK7 has also a long-term negative effect on *FRK1* expression upon pep1 treatment. With these evidences, we suggest that CPK7 plays a complex role downstream of PTI and maintains balance with different defense signals. Although no clear association between CPK7 and several critical PTI components when tested with the BiFC assay, other approaches, such as yeast-two hybrid, for the sake of interactome of CPK7, are necessary for identifying possible direct relationship of CPK7 with key PTI players. For more details of the biochemical and physical function of CPK7, generation of overexpression lines and kinase-dead, EF-hand mutated complementary lines are on-going. By accomplishing these, hopefully we will be able to sketch a fine graph to better define the function of CPK7 in the Arabidopsis defence signaling.
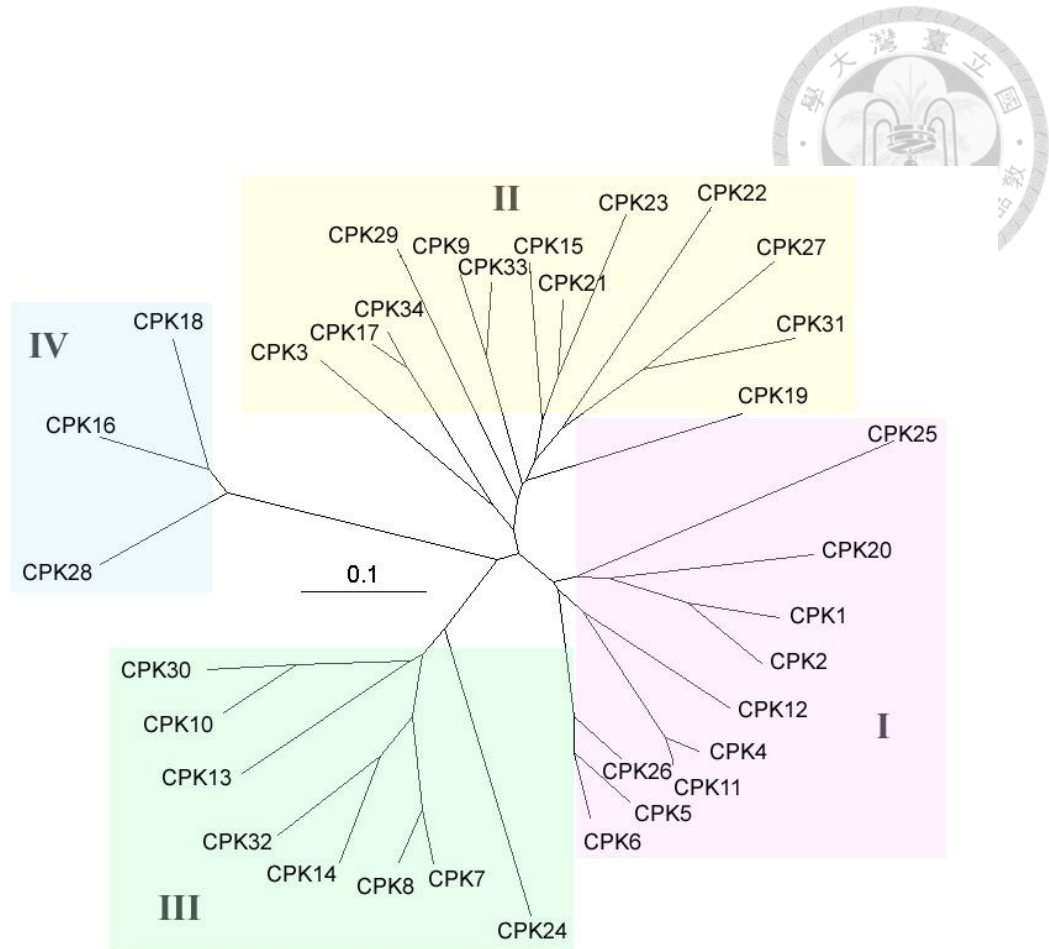
Figure

Figure 1: CPK family in Arabidopsis.

CPK family contains 34 members in 4 groups in Arabidopsis. Adopted from Chen, et
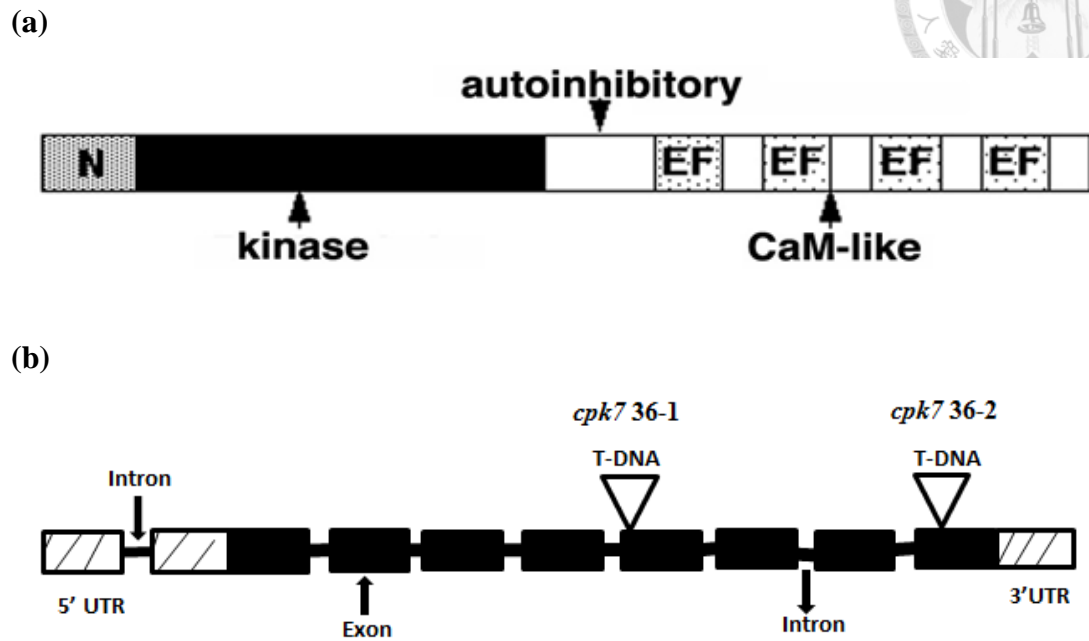
al., 2002.

(a)

(b)

Figure 2: The putative structure of CPK7 and *cpk7* mutants.

(a) CPK7 gene encodes a 535 amino acid residues polypeptide, containing a signal peptide, a N-terminal domain (gray), a conserved serine/threonine kinase domain (black), an autoinhibitory junction region (white) and a C-terminal CamLD (spotted region).

(b) The T-DNA insertion sites for *cpk7* 36-1 and *cpk7* 36-2 in At5g12480. Plant materials were well characterized to be homozygous and could not generate full-length CDS of CPK7 by former member Shweta (Data not shown).
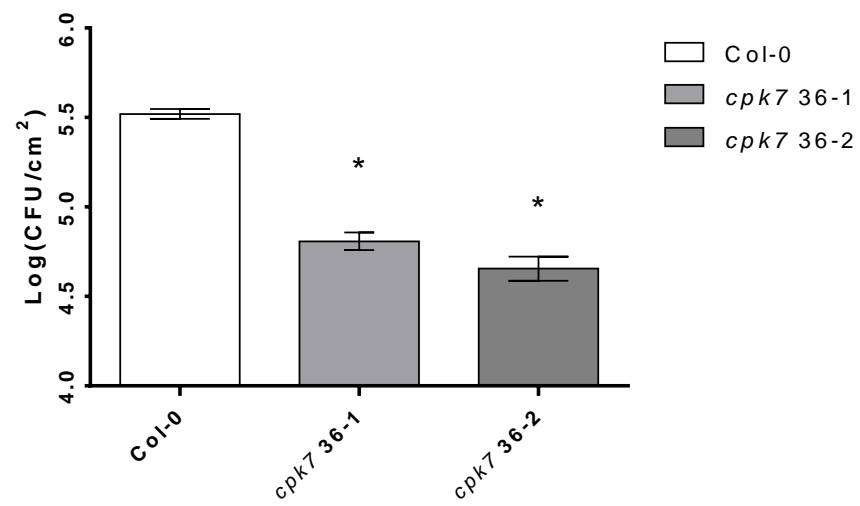
(a)

(b)

Figure 3. Disease symptoms and bacterial titers of Pst DC3000 infected Col-0

and *cpk7* mutant lines

(a) Five-week-old Arabidopsis (Col-0, *cpk7* 36-1 and *cpk7* 36-2) were dip-inoculated

with 2×10^7 cfu/mL *Pst* DC3000. Photos were taken after 3 days. This experiment

was repeated at least 3 times with similar results.

(b) Col-0, *cpk7* 36-1 and *cpk7* 36-2 were dip-inoculated with 1×10^6 cfu/mL *Pst*

DC3000 and bacterial titers were evaluated 2 days later. Data represent 3

independent biological replicates each with 4 technical repeats (n = 12). Asterisks

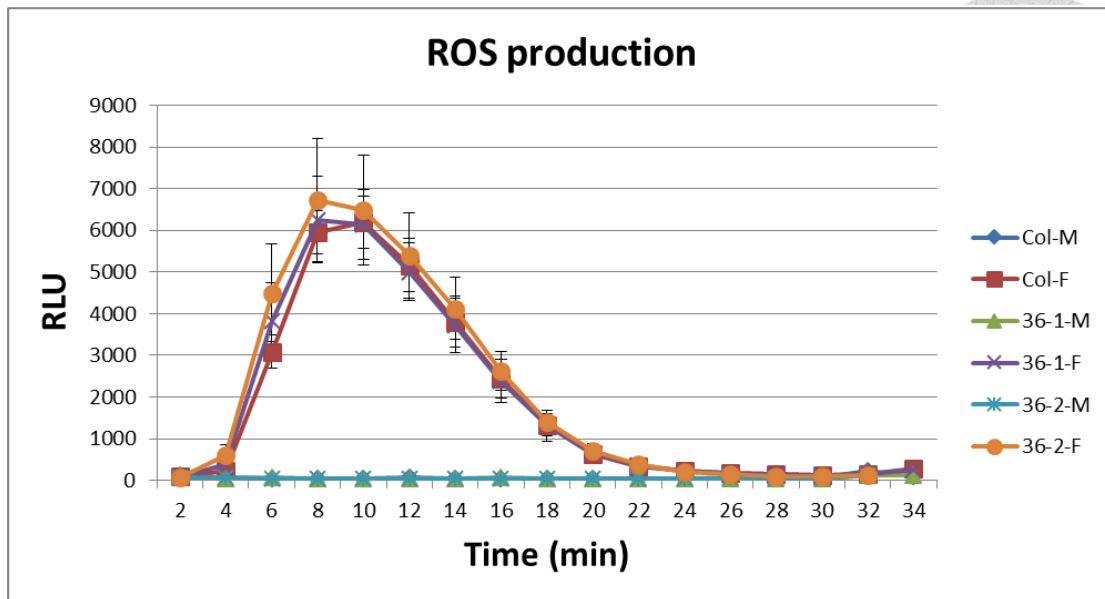indicate a significant difference to WT control on a t test (P < 0.001).

Figure 4. ROS production after flg22 treatment.

Production of ROS in 5-week-old Col-0, *cpk7* 36-1 and *cpk7* 36-2 leaf discs after treatment with 100 nM flg22 (F) as relative light units (RLU). Mock controls (M) were treated with sterilized wate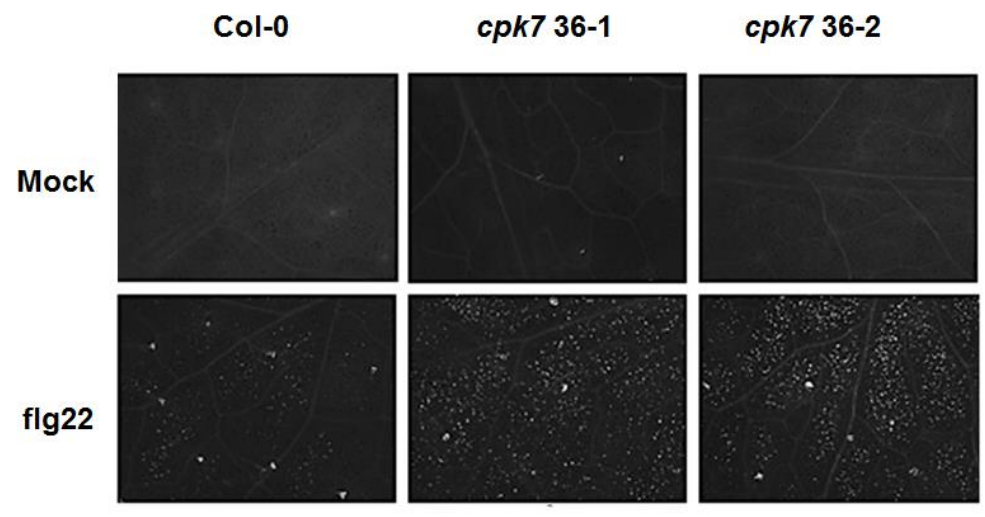r. Values represent averages ± SE (n = 8 for F and 4 for M). Experiments were repeated at least 3 times with similar results.
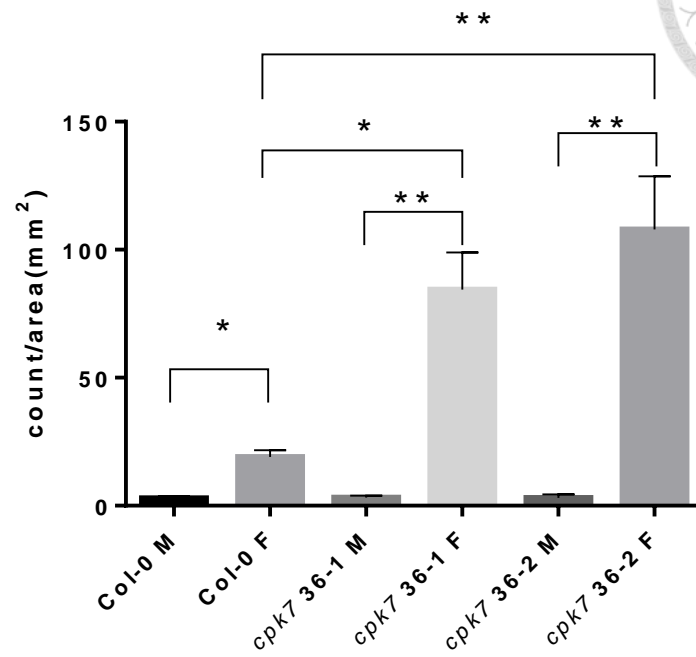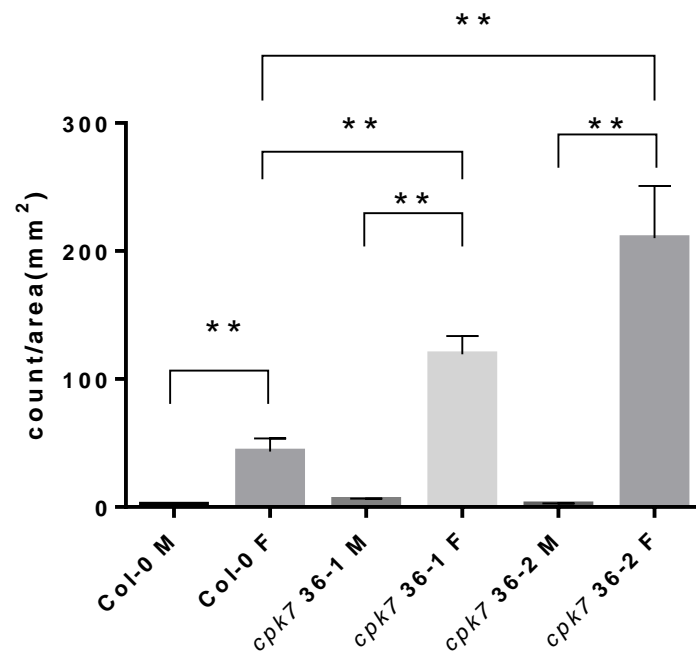
(a)
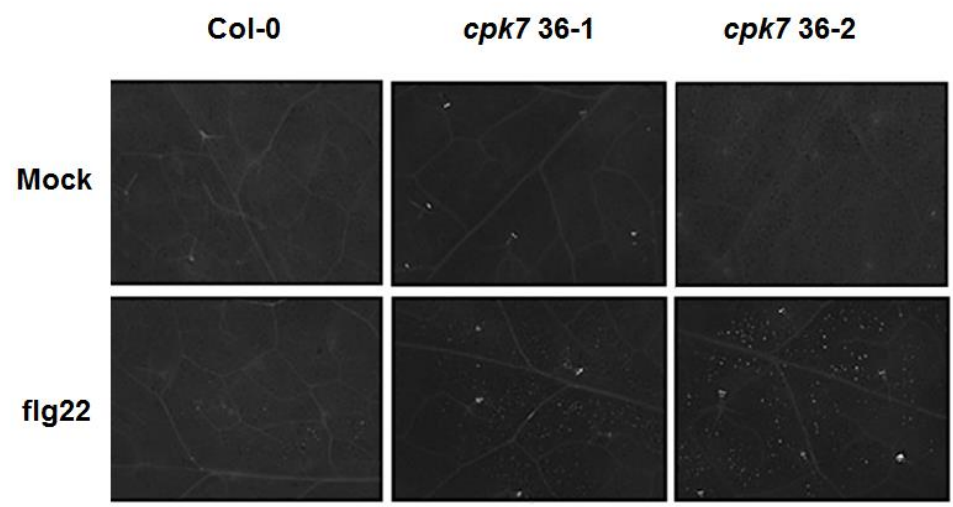
(b)

(c)

(d)

Figure 5. Visualizations and quantifications of callose deposits upon flg22

treatment

Five-week-old Col-0, *cpk7* 36-1 and *cpk7* 36-2 leaves were syringe-infiltrated with 100 nM flg22, and sterilized water were used as mock controls. Samples were harvested 6 h (a) or 9 h (b) later for aniline blue staining. These experiments were repeated 3 times with similar results. Graph represents the average number of callose deposits observed per square millimeter ± SD (n = 12) at 6 h (c) and 9 h (d). Asterisks indicate a significant difference to WT Col-0 treated with flg22 based on a t test (*: $P < 0.005$ and **: $P < 0.001$).
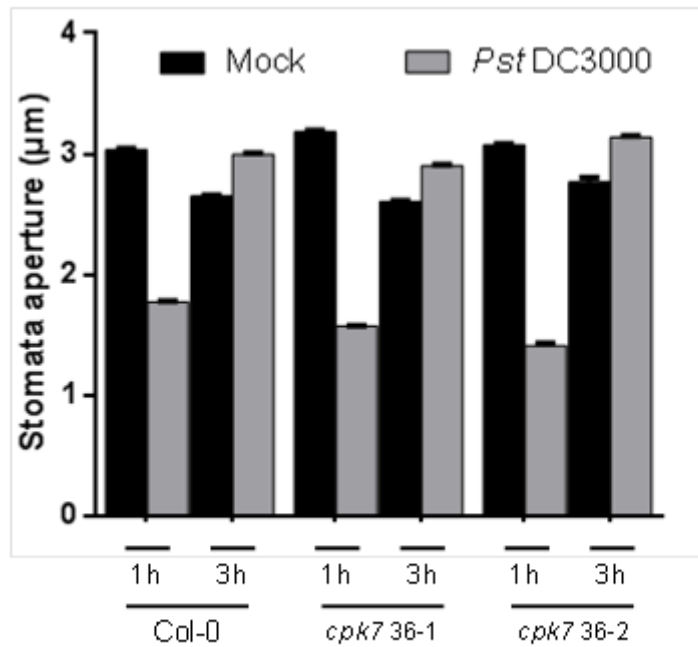
Figure 6: CPK7 in stomatal innate immunity.

Stomatal apertures in leaf epidermal peels from 5-week-old Col-0, *cpk7* 36-1 and *cpk7*

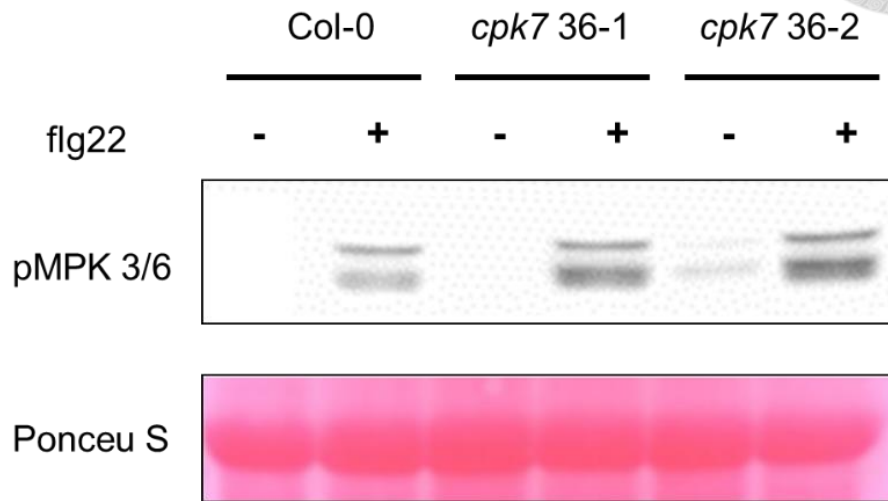36-2 exposed to MES buffer (control) or 1×10^8 cfu/mL *Pst* DC3000 for 1 and 3 h.

Values are shown as means ± SE (n = 80 stomata) of 3 independent biological replicates.

Asterisks indicate a significant difference to Col-0 treatment based on a t test analysis
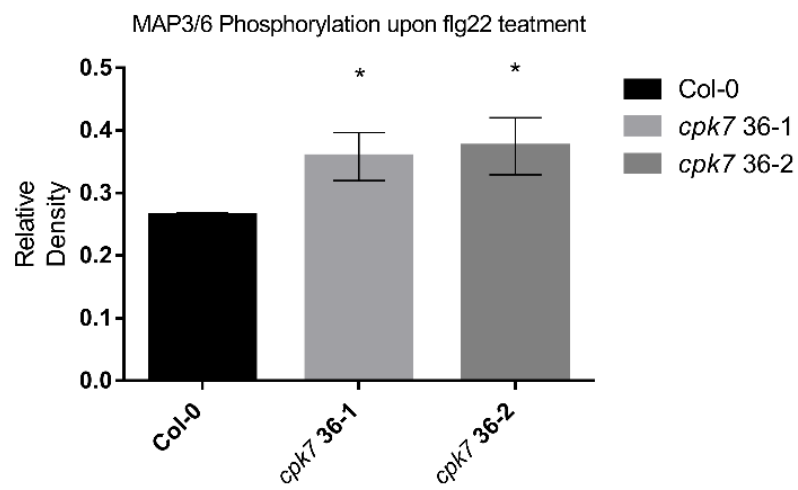
(P < 0.05).

(a)

(b)

Figure 7: MAPK kinase Assay

(a) Nine leaves from 5-week-old Col-0, *cpk7* 36-1 and *cpk7* 36-2 were syringe-infiltrated with 100 nM flg22 (+) and sterilized water (-) for 10 min as shown by immunoblot analysis using phosphor-p44/42 MAK kinase antibody. Immunoblot, top panel; Ponceu S-stained membrane is used to estimate equal loading in each lane, bottom panel. This experiment is one of 2 independent replicates.

(b) Quantification of immunoblot signals to background. Relative densities are average form 2 independent replicates. Asterisks indicate significant differences by t-test ($p<0.05$).

(a)
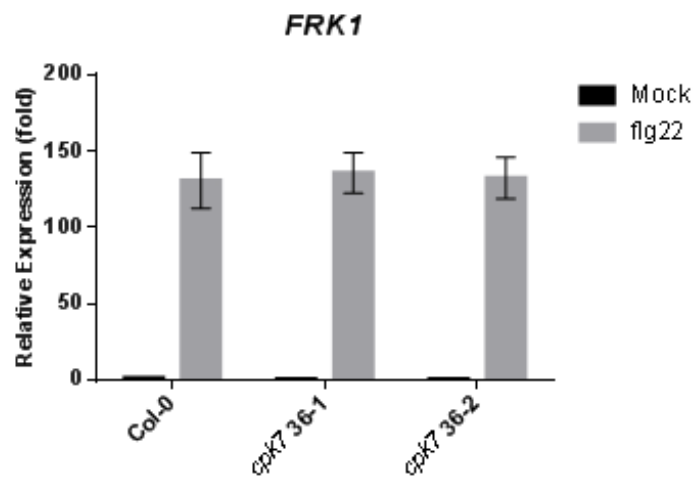
(b)

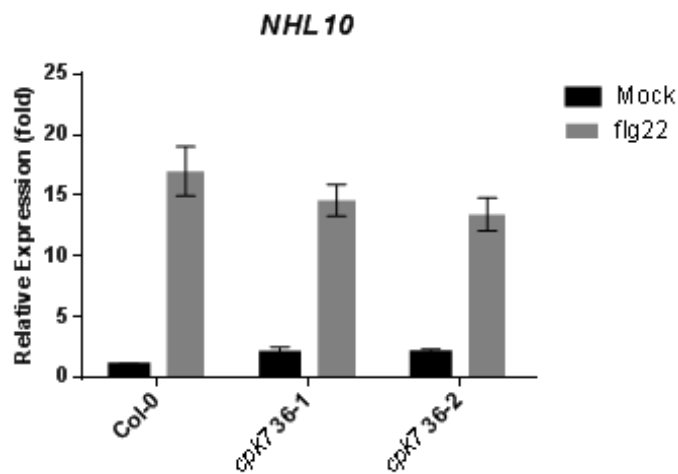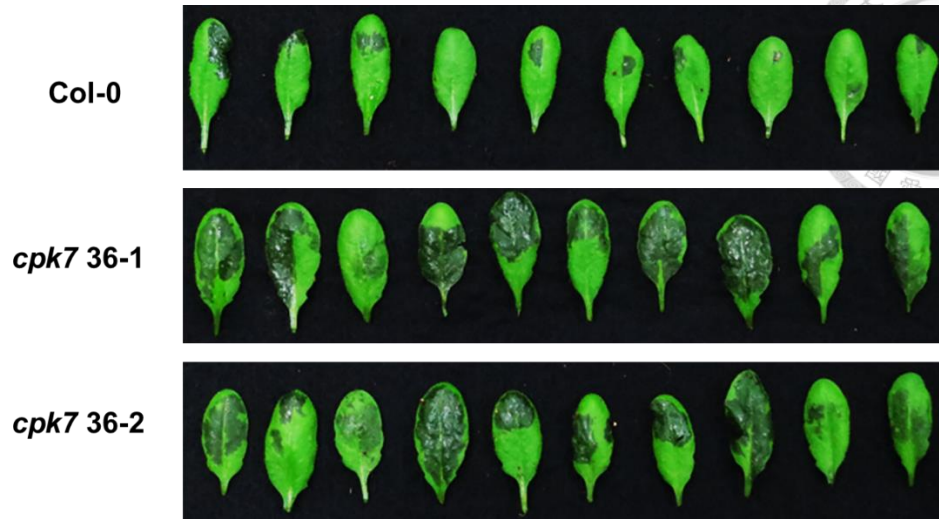**Figure 8. Transcriptional expression of PTI-responsive genes FRK1 and NHL10**

after flg22 treatment.

Relative expression level of *FRK1* (a) or *NHL10* (b) in 5-week-old Col-0, *cpk7* 36-1

and *cpk7* 36-2 were analyzed at 5 h after infiltrated with 100 nM flg22 by qRT-PCR.

UBQ10 was used for normalization. The values are the means ± SE of 3 biological

replicates (n = 9).

(a)

(b)
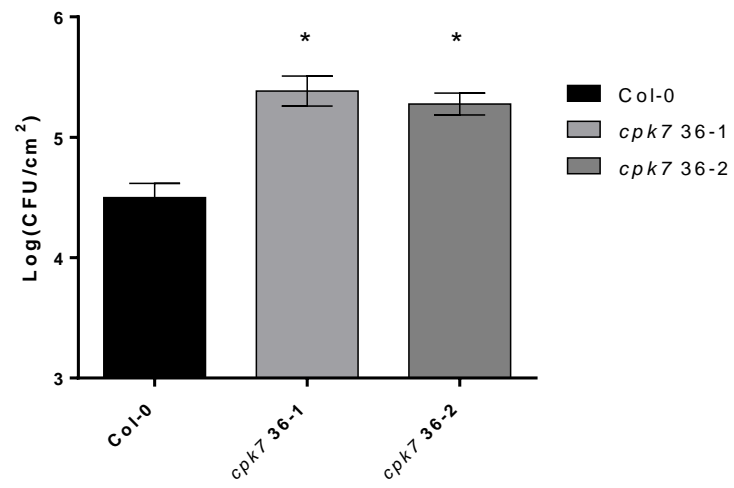
Figure 9.   Disease symptoms and bacterial titers of Pcc infected Col-0 and *cpk7*

mutant lines

(c) Five-week-old Arabidopsis (Col-0, *cpk7* 36-1 and *cpk7* 36-2) were dip-inoculated

with 10^6 cfu/mL *Pcc*. Photos were taken after 2 days. This experiment was repeated

at least 3 times with similar results.

(d) Col-0, *cpk7* 36-1 and *cpk7* 36-2 were dip-inoculated with 10^6 cfu/mL *Pcc* and

bacterial titers were evaluated 2 days later. Data represent 3 independent biological

replicates each with 4 technical repeats (n = 12). Asterisks indicate a significant

difference to WT control on a t test (P < 0.001).

(a)
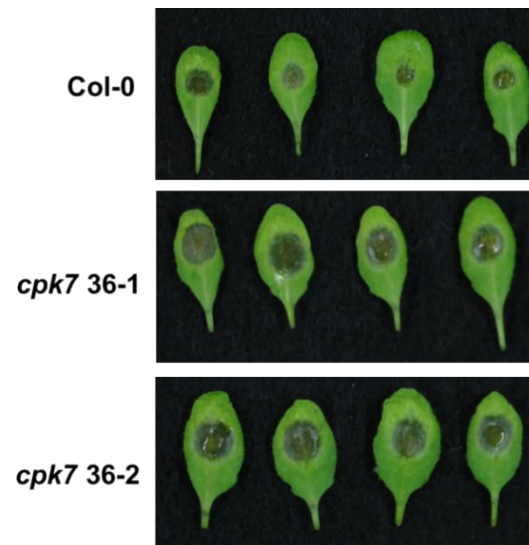
(b)
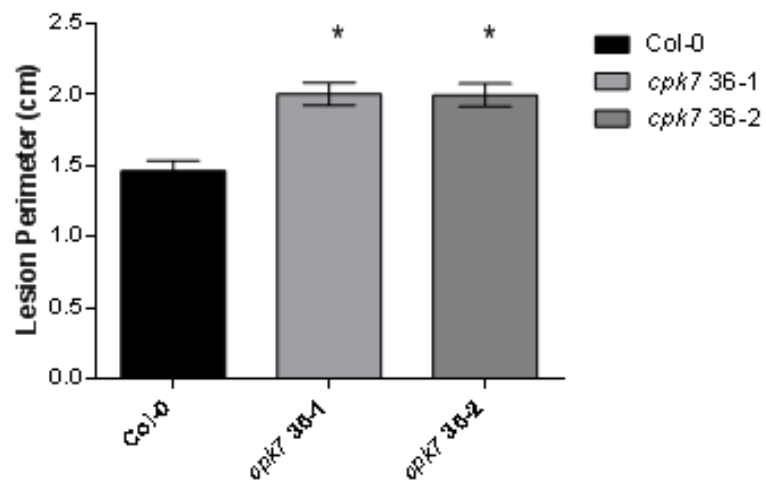
Figure 10: Disease symptoms and lesion perimeter of B. cinerea infected Col-0

and *cpk7* mutant lines

(a) Disease phenotype. *B. cinerea* inoculation was performed on Five-week-old Col-0, *cpk7* 36-1 and *cpk7* 36-2. Plants were inoculated with 8 μL droplets of *B. cinerea* spores (10^5 spores/mL in PDB). Photos were taken at 3 dpi. This experiment was repeated 3 times with similar results.

(b) Lesion perimeter. Measurements were realized at 3 dpi and quantified by Image J. Values are the means ± SE of 3 biological replicates each consisting of 12 technical repeats (n = 36). Asterisks indicate a significant difference to Col-0 control based on a Student's t test (p<0.001).

(a)
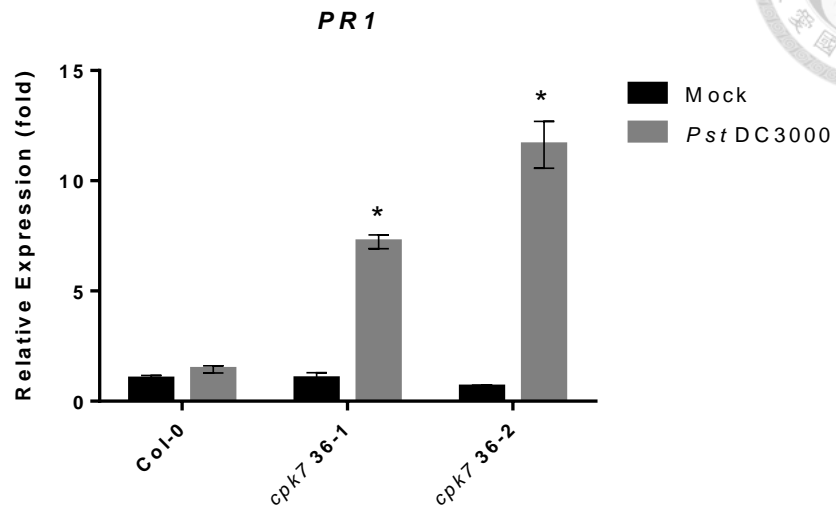
(b)
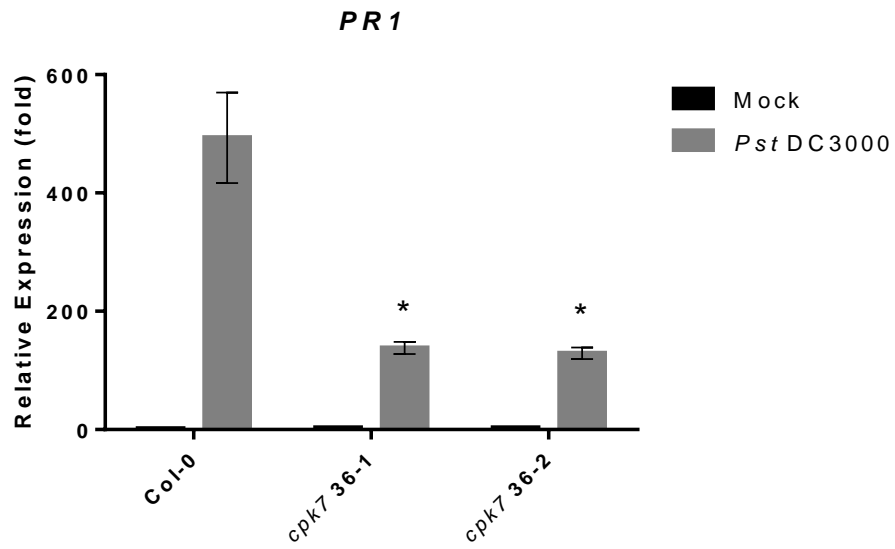
Figure 11: Transcriptional expression of the SA-dependent pathway marker gene

PR1 after Pst DC3000 infiltration.

Relative expression level of *PR1* in leaves from 5-week-old Col-0, *cpk7* 36-1 and *cpk7*

36-2 were analyzed at 5 h (a) and 9 h (b) after infiltrated with 100 nM flg22 by qRT-

PCR. UBQ10 was used for normalization. The values are the means ± SE of 3 technical

repeats (n = 9). The experiments were repeated 3 times with similar results. Asterisks

indicate a significant difference to Col-0 treatment based on a Student's t test (p<0.001).

(a)

PDF1.2

Legend: ■ Mock ▧ *Pcc*

(b)

PDF1.2

Legend: ■ Mock ▧ *B. cinerea*
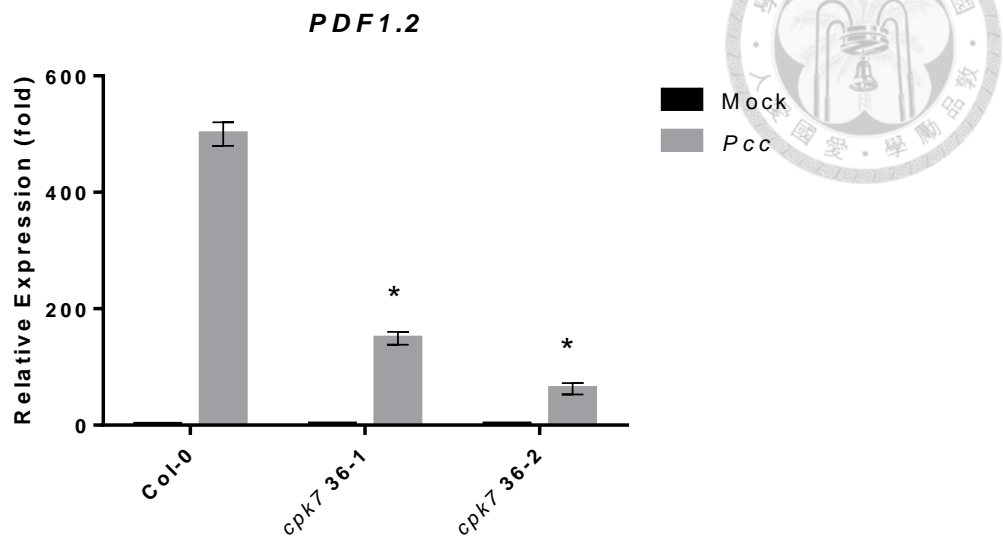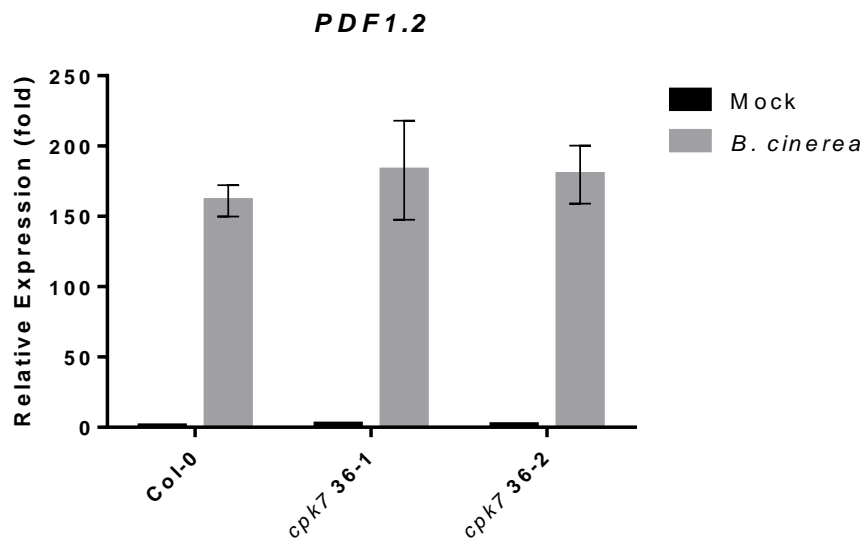
Figure 12: Transcriptional expression of the JA/ET-dependent pathway marker gene PDF1.2 after Pcc and B. cinerea infiltration.

Relative expression level of *PR1* in leaves from 5-week-old Col-0, *cpk7* 36-1 and *cpk7* 36-2 were analyzed after (a) syringe-infiltrated with 10^6 cfu/mL *Pcc* or (b) sprayed with *B. cinerea* (10^5 spores/mL of PDB) 1 day post infection by qRT-PCR. UBQ10 was used for normalization. The values are the means $\pm$ SE of 3 technical repeats (n = 9). The experiments were repeated 3 times with similar results. Asterisks indicate a significant difference to Col-0 treatment based on a Student's t test (p<0.001).

(a)

FRK1

(b)
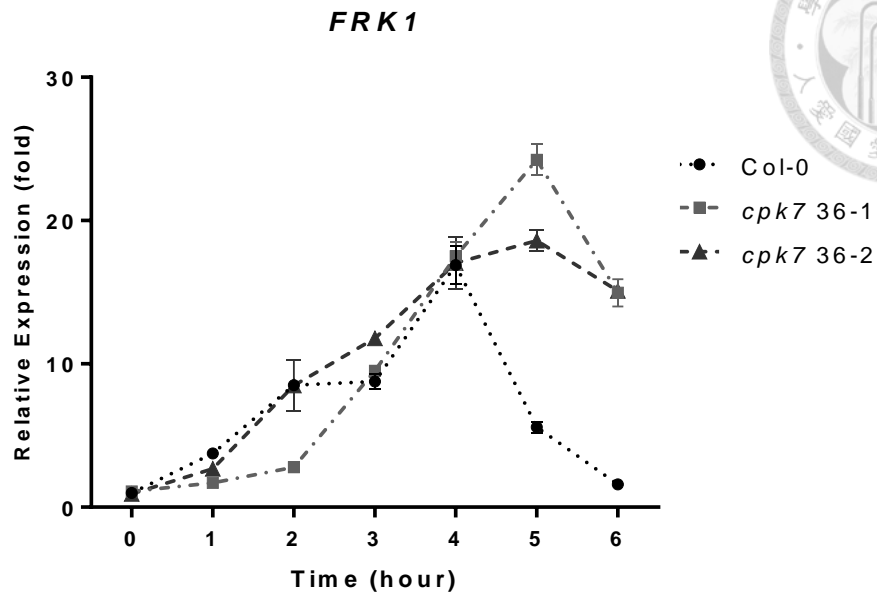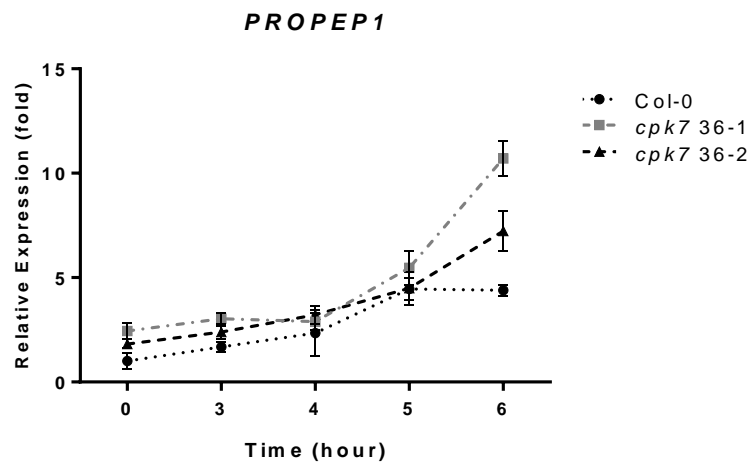
PROPEP1

Figure 13: Transcriptional expression of FRK1 and PROPEP1 upon pep1

treatment.

Relative expression level of *FRK1* (a) or *PROPEP1* (b) in 10-day-old Col-0, *cpk7* 36-

1 and *cpk7* 36-2 were analyzed within 6 h after treated with 0.5 μM pep1 by qRT-PCR.

UBQ10 was used for normalization. The values are the means ± SE of 3 biological

replicates (n = 9). The experiments were repeated 2 times with similar results.
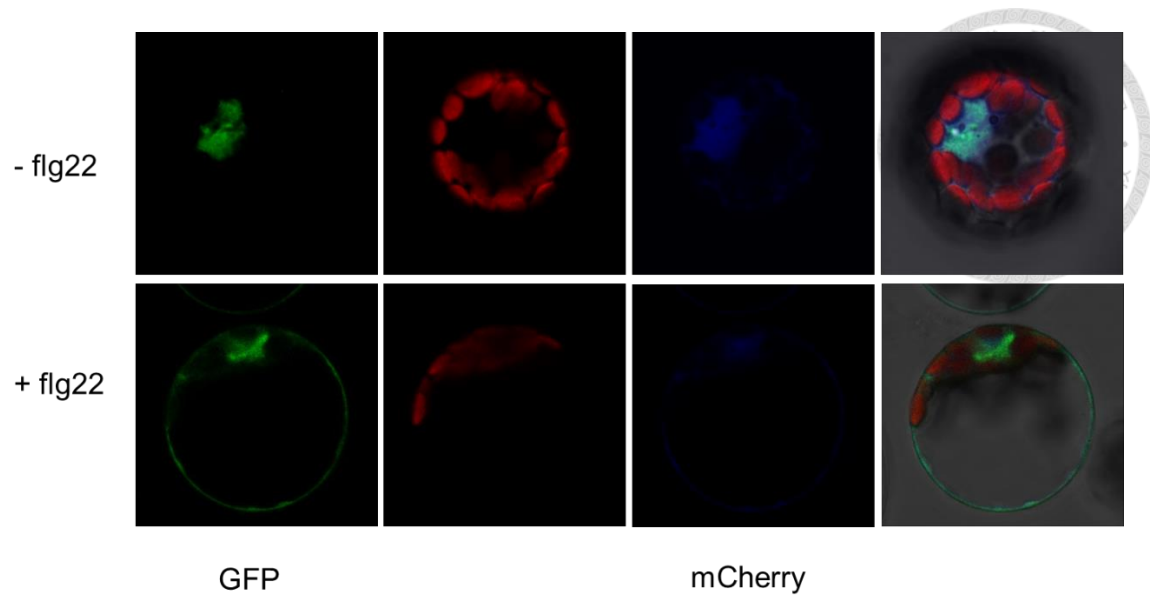
Figure 14: Subcellular localization of CPK7.

Arabidopsis protoplasts were co-transfected with CPK7-GFP and NLS-mCherry, then

treated with 100 nM flg22 (+) and sterilized water (-) for 10 min, and visualized under

a confocal microscope. This experiment is one of 3 independent replicates.

(a)

	YFP	Auto-fluorescence	Bright Field	Merged
AtFLS2-YN +BAK1-YC				
AtBAK1-YN +BIK1-YC				
AtFLS2-YN +CPK7-YC				
AtBAK1-YN +CPK7-YC				
AtCPK7-YN +BIK1-YC				

(b)

	YFP	Auto-fluorescence	Bright Field	Merged
AtPEPR1-YN +PEPR1-YC				
AtPEPR1-YN +CPK7-YC				
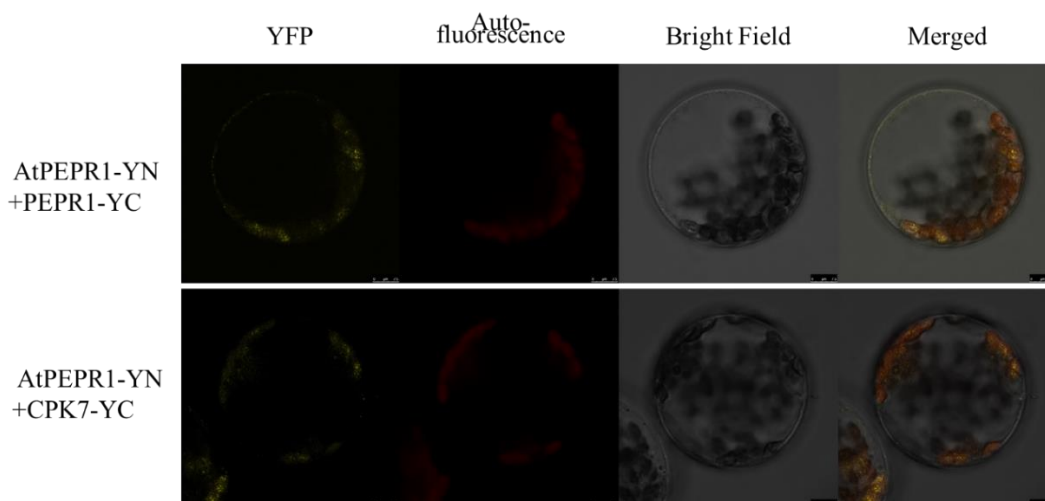
Figure 15: Association of CPK7 with FLS2, BAK1, BIK1 and PEPR1 could not

be observed.

(a) Arabidopsis protoplasts were co-transfected with FLS2-YN, BAK1-YC, BAK1-YN, BIK1-YC, CPK7-YC, and CPK7-YN with different combinations then visualized under a confocal microscope. Photos were taken 15 min after treatment with 200 nM flg22 (except for BAK1-YN + BIK1-YC, what do you mean here, explain how were the conditions for these two proteins). Also, No detectable signals before treatment (data not shown).

(b) Arabidopsis protoplasts were co-transfected with PEPR1-YC or PEPR1-YN, as a positive control, and PEPR1-YN and CPK7-YC. Photos were taken 20 min after treatment with 100 nM pep1 (right?). Scale bars were calibrated to 25 μm. This experiment is one of 2 independent replicates. No detectable signals before treatment (data not shown).

Supplemental table S1. Putative Co-expressing Gene of *LecRK VI.2*

salk name	locus id	given name	tair (annotation)
Salk_019113	AT5g20050	B1 (1-1)	Protein kinase superfamily protein; FUNCTIONS IN: kinase activity; involved in: protein amino acid phosphorylation
Salk_055204C	At4g29740	B1 (15-1)	It encodes a protein whose sequence is similar to cytokinin oxidase/dehydrogenase, which catalyzes the degradation of cytokinins
Salk_127223	At5g12480	B2-36-1	CALMODULIN-DOMAIN PROTEIN KINASE 7, CPK7calmodulin-dependent protein kinase activity, kinase activity, protein kinase activity, protein serine/threonine kinase activity

Supplemental table S2. List of Primers

Primer	sequence
CPK7 cDNA FP	ATGGGGAATTGTTGTGGCA
CPK7 cDNA RP	CAATGAACCATCTCTCATTAACTTGAG
UBQ FP	AAAGAGATAACAGGAACGGGAAC
UBQ RP	GGCCTTGTATAATCCCTGATGAA
PR1 FP	AAAACTTAGCCTGGGGTAGCGG
PR1 RP	CCACCATTGTTACACCTCACTTTG
PDF1.2a FP	AATCTTTGGTGCTAAATCGTGTG
PDF1.2a RP	CAACGGGAAAATAAACATTAAAA
FRK1 FP	GCCAACGGAGACATTAGAG
FRK1 RP	CCATAACGACCTGACTCATC
NHL10 FP	TTCCTGTCCGTAACCCAAAC
NHL10 RP	CCCTCGTAGTAGTAGGCATGAGC
PEPR1 CDS FP	ATGAAGAATCTTGGGGGGTTG
PEPR1 CDS RP	CCGAACTGAATCAGAGGAGCA
AtproPep1 FP	CTTATCAGATCTCAATGGAGAAATC
AtproPep1 RP	CAATGTAACTTAAAGTGCCTAATTATG
ERF1 FP	CGAGAAGCTCGGGTGGTAGT
ERF1 RP	GCCGTGCATCCTTTTCC

FP: forward primer. RP: reverse primer.

Supplemental Figure S1: Transcriptional expression of *ERF1* upon ACC treatment.

Relative expression level *ERF1* in 5-week-old Col-0, *cpk7* 36-1 and *cpk7* 36-2 were analyzed within 6 h after treated with 0.2 mM ACC by qRT-PCR. UBQ10 was used for normalization. The values are the means ± SE of 3 biological replicates (n = 9). The experiments were repeated only 2 times with similar results.
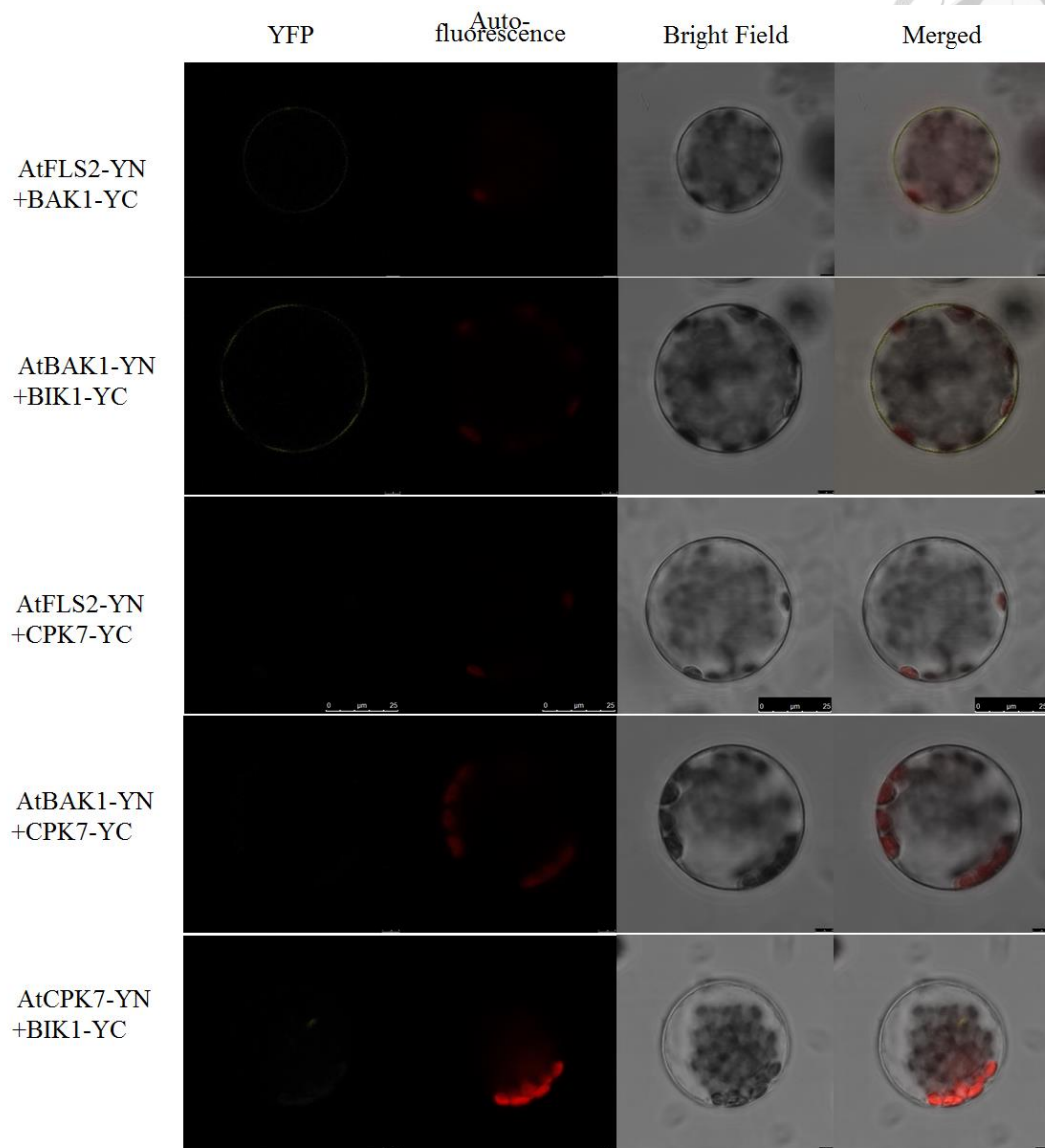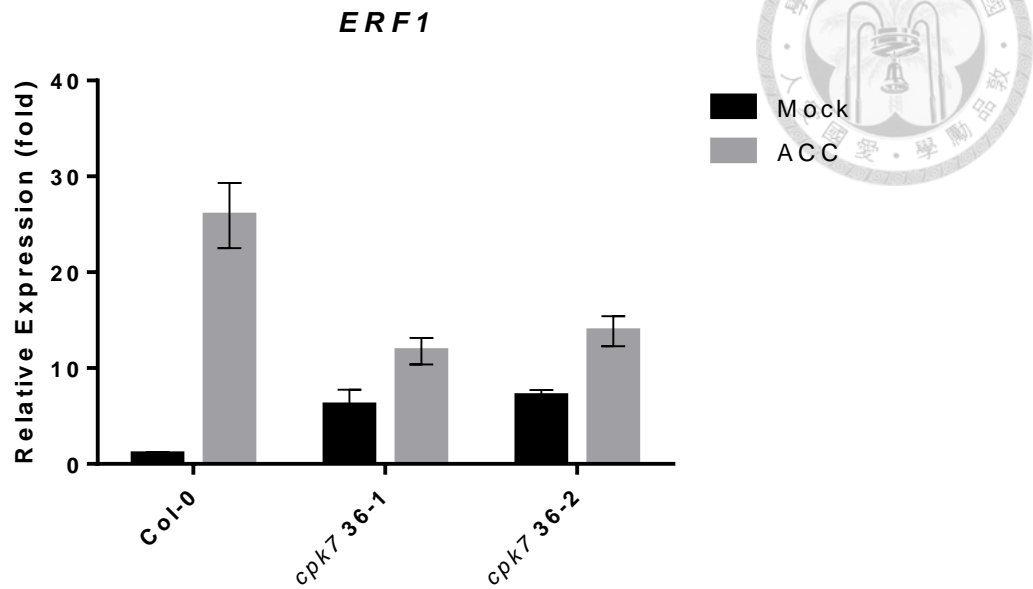
References

Asai, T., Tena, G., Plotnikova, J, Willmann, M.R., Chiu, W.L., Gomez-Gomez, L., Boller T, Ausubel, F.M., and Sheen, J. (2002). MAP kinase signalling cascade in Arabidopsis innate immunity. Nature 415: 977-83.

Ausubel, F.M. (2005). Are innate immune signaling pathways in plants and animals conserved? Nat. Immunol. 6: 973–979

Bari, R. and Jones, J.D. (2009). Role of plant hormones in plant defence responses. Plant Mol. Biol. 69: 473-488.

Bartels, S., Lori, M., Mbengue, M.,van Verk, M., Klauser, D., Hander, T., Robatzek, S., and Boller, T. (2013). The family of AtPeps and their precursors in Arabidopsis: Differential expression and localization but similar induction of pattern-triggered immune responses. Journal of Experimental Botany In Press.

Boller, T., and Felix, G. (2009). A renaissance of elicitors: Perception of microbe-associated molecular patterns and danger signals by patternrecognition receptors. Annu. Rev. Plant Biol. 60: 379–406.

Boller, T., and He, S.Y. (2009). Innate immunity in plants: An arms race between pattern recognition receptors in plants and effectors in microbial pathogens. Science 324: 742–744.

Bostock, R.M. (2005). Signal crosstalk and induced resistance: Straddling the line between cost and benefit. Annual Review of Phytopathology 43: 545-580.

Boudsocq, M. (2012). Characterization of Arabidopsis calcium dependent protein kinases: activated or not by calcium? Biochem. J. 447: 291–299

Boudsocq M., and Sheen J. (2013). CDPKs in immune and stress signaling. Trends Plant Sci. 18: 0-40

Boudsocq, M., Willmann, M.R., McCormack, M., Lee, H., Shan, L., He, P., Bush, J., Cheng, S.H., and Sheen, J. (2010). Differential innate immune signalling via Ca(2+) sensor protein kinases. Nature 464: 418-422.

Cheng, S.H., Willmann, M.R., Chen, H.C., and Sheen, J. (2002). Calcium signaling through protein kinases. The Arabidopsis calcium-dependent protein kinase gene family. Plant Physio. 129: 449-485

Chen, X.-Y., and Kim, J.-Y. (2014). Callose synthesis in higher plants. Plant Signal Behav. 4: 489-492

Chinchilla, D., Zipfel, C., Robatzek, S., Kemmerling, B., Nurnberger, T., Jones, J.D., Felix, G., and Boller, T. (2007). A flagellin-induced complex of the recep-tor FLS2 and BAK1 initiates plant defence. Nature 448: 497-500.

Christodoulou, J., Malmendal, A., Harper, J.F. and Chazin, W.J. (2004) Evidence for differing roles for each lobe of the calmodulin-like domain in a calcium-dependent protein kinase. J. Biol. Chem. 279: 29092–29100

Coca, M. and San Segundo, B. (2010). AtCPK1 calcium-dependent protein kinase mediates pathogen resistance in Arabidopsis. Plant J. 63: 526–540

de Torres Zabala M., Bennett M.H., Truman W.H., and Grant M.R. (2009). Antagonism between salicylic and abscisic acid reflects early host-pathogen conflict and moulds plant defence responses. Plant J. 59: 75-86
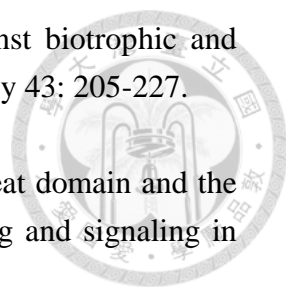
DeFalco, T.A., Bender, K.W., and Snedden, W.A. (2010) Breaking the code: Ca2+ sensors in plant signalling. Biochem. J. 425: 27–40.

Dong, C., Davis, R.J., and Flavell, R. (2002). MAP kinases in the immune response. Annual Review of Immunology 20: 55-72.

Downie, J.A. (2014). Calcium signals in plant immunity: a spiky issue. New Phytol. 204: 33-5.

Feys, B.J., Moisan, L.J., Newman, M., and Parker, J. (2001). Direct interaction between the Arabidopsis disease resistance signaling proteins, EDS1 and PAD4. The EMBO J. 20: 5400-5411.

Gao, X., Cox, K.L., and He P. (2014). Functions of Calcium-Dependent Protein Kinases in Plant Innate Immunity. Plants 3: 160-176

Glazebrook, J. (2005). Contrasting mechanisms of defense against biotrophic and necrotrophic pathogens. Annual Review of Phytopathology 43: 205-227.

Gomez-Gomez, L. (2001). Both the extracellular leucine-rich repeat domain and the kinase activity of FLS2 are required for flagellin binding and signaling in Arabidopsis. Plant Cell 13: 1155-1163.

Greenberg, J.T. and Yao, N. (2004). The role and regulation of programmed cell death in plant-pathogen interactions. Cellular Microbiology 6: 201-211

Huffaker, A., and Ryan, C.A. (2007). Endogenous peptide defense signals in Arabidopsis differentially amplify signaling for the innate immune response. Proc Natl Acad Sci. USA. 104: 10732 – 10736

Jones, J.D.G., and Dangl, J.L. (2006). The plant immune system. Nature 444: 323–329.

Kanchiswamy, C.N. (2010). Regulation of Arabidopsis defense responses against Spodoptera littoralis by CPK-mediated calcium signaling. BMC Plant Biol. 10: 97

Kang, G.H., Son, S., Cho, Y.H., and Yoo, S.D. (2015). Regulatory role of BOTRYTIS INDUCED KINASE1 in ETHYLENE INSENSITIVE3-dependent gene expression in Arabidopsis. Plant Cell Rep.

Keppler L.D., Baker C.J., and Atkinson M.M. (1989). Active oxygen production during a bacteria-induced hypersensitive reaction in tobacco suspension cells. Phytopathology 79: 974-978

Li, G., Boudsocq, M., Hem, S., Vialaret, J., Rossignol, M., Maurel, C., and Santoni, V. (2015). The calcium-dependent protein kinase CPK7 acts on root hydraulic conductivity. Plant Cell Environ. 38: 312-20.

Melotto, M., Underwood, W., Koczan, J., Nomura, K., and He, S.Y. (2006). Plant stomata function in innate immunity against bacterial invasion. Cell 126: 969-980.

Misra, B.B., Acharya, B.R., Granot, D., Assmann, S.M., and Chen, S. (2015). The guard cell metabolome: functions in stomatal movement and global food security. Front Plant Sci. 6:334.

Monaghan J., Matschi S., Romeis T., and Zipfel C. (2015). The calcium-dependent protein kinase CPK28 negatively regulates the BIK1-mediated PAMP-induced calcium burst. Plant Signal Behav. 10: e1018497.

Petersen M., Brodersen P., Naested H., Andreasson E., Lindhart U., Johansen B., Nielsen H.B., Lacy M., Austin M.J., and Parker J.E. (2000). Arabidopsis MAP kinase 4 negatively regulates systemic acquired resistance. Cell 103:1111-1120.

Pieterse, C.M., Leon-Reyes, A., van Endt, S., and van Wees, S. (2009). Networking by small-molecule hormones in plant immunity. Nature Chem. Bio. 5: 308-316.
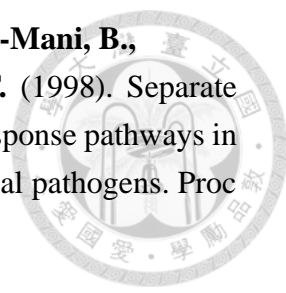
Pieterse, C.M., D. van der Does, C. Zamioundis, A. Leon-Reyes, and S. van Wees (2012). Hormonal modulation of plant immunity. Annual Rev. of Cell and Developmental Biology 28: 489-521

Romeis T, and Herde M. (2014). From local to global: CDPKs in systemic defense signaling upon microbial and herbivore attack. Curr Opin Plant Biol. 20:1-10.

Ross, A., Yamada, K., Hiruma, K., Yamashita-Yamada, M., Lu, X., Takano, Y., Tsuda, K. and Saijo, Y. (2014). The Arabidopsis PEPR pathway couples local and systemic plant immunity. The EMBO J. 33: 62-75

Sanders, D., Pelloux, J., Brownlee, C., Harper, J.F. (2002) Calcium at the crossroads of signaling. Plant Cell 14: S401–S417.

Singh P., Kuo Y.C., Mishra S, Tsai C.H., Chien C.C., Chen C.W., Desclos-Theveniau M., Chu P.W., Schulze B, Chinchilla D, Boller T., and Zimmerli L. (2012). The lectin receptor kinase-VI.2 is required for priming and positively regulates Arabidopsis pattern-triggered immunity. Plant Cell 24: 1256-70.

Thomma, B.P.H.J, Eggermont, K., Penninckx, I.A.M.A., Mauch-Mani, B., Vogelsang, R., Cammue, B.P.A., and Broekaert, W.F. (1998). Separate jasmonate dependent and salicylate-dependent defense-response pathways in Arabidopsis are essential for resistance to distinct microbial pathogens. Proc Natl Acad Sci. 95:15107-15111.

Van Verk, M.C., Gatz, C., and Linthorst, H.J.M. (2009). Transcriptional Regulation of Plant Defense Responses. In Advances in Botanical Research, L.C.V. Loon, ed (Academic Press), pp. 397-438.

Weljie, A.M. and Vogel, H.J. (2004) Unexpected structure of the Ca2+ -regulatory region from soybean calcium-dependent protein kinase-α. J. Biol. Chem. 279: 35494–35502

Yamaguchi, Y., Huffaker, A., Bryan, A., Tax, F., and Ryan, C. (2010). PEPR2 is a second receptor for the Pep1 and Pep2 peptides and contributes to defense responses in Arabidopsis. Plant Cell 22: 508-522.

Yan, J.B., Zhang, C., Gu, M., Bai, Z., Zhang, W., Qi, T., Cheng, Z., Peng, W., Lou, H., Nan, F., Wang, Z., and Xie D. (2009). The Arabidopsis CORONATINE INSENSITIVE1 protein is a jasmonate receptor. Plant Cell 21: 2220-2236.

Yoo, S.D., Cho, Y.H., and Sheen, J. (2007). Arabidopsis mesophyll protoplasts: a versatile cell system for transient gene expression analysis. Nat Protoc 2: 1565-1572.

Zimmerli, L., Metraux, J.P., and Mauch-Mani, B. (2001). beta-Aminobutyric acid-induced protection of Arabidopsis against the necrotrophic fungus Botrytis cinerea. Plant Physiol. 126: 517-523.

Zipfel, C., Robatzek, S., Navarro, L., Oakeley, E., Jones, J.D., Felix, G., and Boller, T. (2004). Bacterial disease resistance in Arabidopsis through flagellin perception. Nature 428: 764-767.